ESC-TR-93-211

Technical Report
981

A Compact, Portable EHF/SHF Antenna for Advanced SCAMP

J.C. Lee

22 September 1993

Lincoln Laboratory

MASSACHUSETTS INSTITUTE OF TECHNOLOGY

LEXINGTON, MASSACHUSETTS

Prepared for the Department of the Army under Air Force Contract F19628-90-C-0002.

This report is based on studies performed at Lincoln Laboratory, a center for research operated by Massachusetts Institute of Technology. The work was sponsored by the Department of the Army under Air Force Contract F19628-90-C-0002.

The ESD Public Affairs Office has reviewed this report, and it is releasable to the National Technical Information Service, where it will be available to the general public, including foreign nationals.

This technical report has been reviewed and is approved for publication.

FOR THE COMMANDER

Gary Tatungian
Administrative Contracting Officer
Directorate of Contracted Support Management

MASSACHUSETTS INSTITUTE OF TECHNOLOGY
LINCOLN LABORATORY

A COMPACT, PORTABLE EHF/SHF ANTENNA FOR ADVANCED SCAMP

J.C. LEE
Group 63

TECHNICAL REPORT 981

22 SEPTEMBER 1993

LEXINGTON MASSACHUSETTS

6 October 1993

ERRATA

Document: Technical Report 981
A Compact, Portable EHF/SHF Antenna for Advanced SCAMP
22 September 1993

The three occurrences of "*A-A*" on page 9 should read "*A-A´*."

In Section 7.1, page 37, the word "mixture" in the first line should be "fixture."

Reference 4 on page 49 should read "J.L. Lee," not "J.C. Lee."

Please mark your copy accordingly.

Publications Office
MIT Lincoln Laboratory
P.O. Box 73
Lexington, MA 02173-9108

ABSTRACT

SCAMP is a small, single-channel, antijam, man-portable terminal used for extremely high frequency (EHF) satellite communication. Since its development in 1987, it has repeatedly demonstrated successful communication through the EHF packages on the FLTSAT-7 and -8 Navy communications satellites.

Advanced SCAMP is the second generation small terminal, highly elevated in performance and significantly reduced in weight, currently being developed at Lincoln Laboratory. Pertinent parameters are its 30-lb total weight, 75- to 2,400-bps data rate, and 24-in antenna aperture.

Starting with the basic dual-band feed developed for another application, a compact, high-performance, EHF dual-band ring-focus feed with an elliptical subreflector was developed for a displaced axis parabolic reflector. This reflector is made up of six lightweight deployable petals for portability.

The feed weighs less than 1 lb, and the reflector weighs 2.6 lb. The measured added loss due to imperfections of the petal reflector for the 44.5- and 20.7-GHz bands are 0.3 and 0.1 dB, respectively. An overall antenna efficiency of about 65% and 55% in the Q- and K-bands, respectively, was achieved.

Antenna and feed design considerations, measured performance, and other possible applications for this antenna are discussed.

ACKNOWLEDGMENTS

The author acknowledges the support of W.C. Cummings, D.M. Snider, R.F. Bauer; technical discussions with W. Rotman and A. Dion; the mechanical design of T. Lunny; the measurement assistance of R. Burns, J. McCrillis, T. Arbo, J. Perry, D. Besse; and the fabrication skill of G. Willman.

TABLE OF CONTENTS

LIST OF ILLUSTRATIONS

LIST OF ILLUSTRATIONS (Continued)

LIST OF TABLES

1. INTRODUCTION

Advanced SCAMP (single-channel, antijam, man-portable) is a small, lightweight, extremely-/super-high frequency (EHF/SHF) satellite communication terminal that is easily transported. Advanced SCAMP (ASCAMP) weighs approximately 30 lb, communicates at data rates ranging from 75 to 2,400 bps at high hop rate, and uses a 24-in diameter antenna with six removable reflector petals.

The ASCAMP antenna is a centrally fed displaced axis reflector with a ring-focus dual-band feed. The antenna design was selected to minimize weight and maximize gain in both the up- and downlink frequency bands, while accommodating hardware that holds the detachable reflector petals.

Using the dual-band feed designed for SCOTT (single channel objective tactical terminal) ADM (advanced design model) as a starting point, a compact, high-performance, EHF/SHF dual-band (44.5/20.7 GHz) feed with a ring focus was developed. The ring focus is generated by a subreflector, the reflecting surface of which is the revolution of part of a tilted ellipse. The ring focus matches the focal ring of the displaced axis parabolic reflector. For portability the reflector is made of six lightweight, removable petals. The feed weighs less than 1 lb, and the reflector weighs 2.6 lb. Overall antenna efficiencies of better than 55% in the 20.7-GHz receive frequency band and 65% in the 44.5-GHz transmit frequency band were achieved. (This includes an added loss due to imperfections in the reflector shape of 0.1 and 0.3 dB for the two bands.) As the reflector assembly design progressed from original concept through first experimental prototypes and finally to limited production (about 50 petals), many design improvements were implemented. The improvements increased electrical performance, made petal production easier and less expensive; and made assembly and disassembly easier, less bothersome, and physically more reliable. This report discusses all aspects of the antenna and feed design, mechanical fabrication details, and measured performance of the ASCAMP antennas as they evolved.

2. CONFIGURATION CONSIDERATIONS

2.1 DUAL-BAND ANTENNA

The dual-frequency band ratio γ is defined as the quotient of the center frequency of the high-frequency band and the center frequency of the low-frequency band. For γ close to 1, a single broadband antenna and feed can be used. The two "bands" can be easily separated by the use of filters or polarization diplexers. For γ much larger than 1, many systems will utilize two antennas—one for the low- and one for the high-frequency band. Generally, the low-frequency band antenna dominates in size. The high-frequency band feed and antenna, being relatively small in comparison, contribute little to overall size and weight. The two ASCAMP bands are Q (43.5 to 45.5 GHz) and K (20.2 to 21.2), and $\gamma = 2.15$.

Three approaches to a dual-band antenna were considered for $\gamma = 2.15$:

(1) Dual antennas (one for each band)

(2) Single main reflector with a dichroic subreflector and two feeds

(3) Single main reflector with a single dual-band feed.

The first approach is elementary and straightforward. Because the two bands are electrically independent, the RF design of each can be individually optimized; however, the result is a bulky and unwieldy structure.

The second approach (Lindberg [1]) relies on a dichroic surface to align the illumination from two separate feed horns onto the main reflector. For the low-frequency band the feed is located at the prime focus of the main reflector looking through the dichroic subreflector. For the high-frequency band the feed is located at the focus of the dichroic subreflector, and the antenna acts as a Cassegrain antenna. The dichroic surface consists of an array of numerous metallic elements, resonant at 44 GHz, on a curved dielectric substrate. The development and production of such a surface is relatively difficult and costly.

The third approach results in the most compact design. The crucial component is the dual-band feed. (The high-performance feed designed for the SCOTT ADM served as a starting point in its development.)

2.2 ANTENNA REQUIREMENTS

To meet ASCAMP development goals, antenna design criteria were:

- *Portability and/or Deployability.* For ease of transport the size of the complete terminal when stowed for travel was limited to that of airline carry-on luggage; however, to obtain the desired communication performance, a 24-in diameter antenna was necessary. Because the required antenna aperture size is larger than can be packaged in the required volume, the reflector was segmented, and easy assembly/disassembly was a major design consideration.
- *High Performance in Both Bands.* Because inefficient antennas are larger than those that are efficient and operate at the same frequency with the same gain, an effort was made to maximize

overall antenna efficiency by choosing the proper reflector shape and keeping tight surface tolerances. The design goal was for high gain, about 46 dBi for the 43.5- to 45.5-GHz uplink (Q) band and 39 dBi for the 20.2- to 21.2-GHz downlink (K) band, with high efficiency (>50% for both), low losses, good impedance match, and high isolation between the two bands.

2.3 ANTENNA REALIZATION

The high antenna gain requirement stipulates an aperture antenna. The gain of an aperture is given by

$$G_0 = \eta\left(\frac{\pi D}{\lambda}\right)^2 \quad . \tag{1}$$

where η is the overall antenna efficiency, D is the aperture diameter, and λ is the wavelength. For a given frequency the desired gain is achieved by choosing a large-enough aperture diameter. To minimize D, η should be as large as possible.

High gain implies a narrow antenna beamwidth, which in turn requires good antenna pointing accuracy. Close to the boresight peak, the beam pattern of a circular symmetric aperture antenna can be approximated by the function

$$G(\theta) = G_0 \; e^{-0.69\left(\frac{\theta}{\theta_3}\right)^2} \tag{2}$$

where θ_3 ($\theta_3 = 30\ \lambda/D$) is half the 3-dB beamwidth. Assuming $\eta = 0.6$, for 44.5 GHz the antenna gain variation as a function of pointing error in degrees for several aperture sizes is given in Figure 1. This figure shows that a 24-in aperture has a gain over 46 dBi for a pointing error up to 0.2 deg. Thus a 24-in aperture provides the required gain with the expected performance of the pointing system.

2.4 APERTURE TYPES

There are three types of practical high-gain aperture antennas: arrays, lenses, and reflectors. This section examines each and its suitability for the present ASCAMP application.

Array antennas can be made to conform to a given surface contour. With electronic switching and/or phase-shifting elements, the antenna beam can be electronically pointed. EHF phased arrays require small, highly precise, complex circuits that are technically difficult and expensive to fabricate. Even for fixed-beam applications, the requirement of a large number of antenna elements and their related feed network make such an antenna expensive. Klaus [2] describes a 32- × 32-element array operating at 38 GHz with 35% efficiency and 29-dBi gain. These performance parameters are well below those needed for ASCAMP. Furthermore, ASCAMP requires dual-band operation to minimize size. The author is not aware that any satisfactory dual-band array has been reported to date; therefore, array antenna designs were not considered viable candidates for this application.

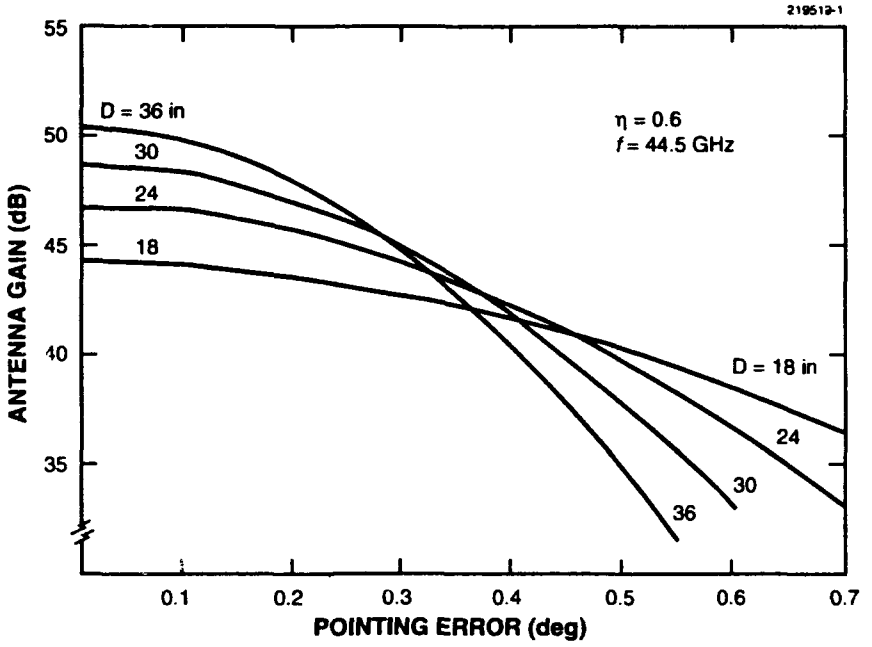

Figure 1. Antenna gain versus pointing error.

Lens antennas utilize refraction at two surfaces to form the beam. The lens must have a definite thickness. Thus lens antennas tend to be bulky. If a lens is made of a dielectric material, it may be heavy (an 18-in Rexolite lens may weigh as much as 20 lb). Also, dielectric loss reduces gain. If the lens is made of thin-walled waveguide, it is likely to be narrowband. In addition, precise fabrication requirements make it expensive. Impedance matching at the lens surfaces and zoning to save weight result in reduced performance for dual-band operation. For these reasons lens antennas were not considered suitable for ASCAMP application.

In contrast, reflector antennas utilize reflection from one conducting surface to form the beam. In principle the surface can be made very thin and thus can be lightweight and simple. The required reflector surface shape deviation tolerance to minimize loss in gain is proportional to wavelength. At EHF a high surface accuracy is required. Reflector surface efficiency due to small random surface roughness η_s and the corresponding gain loss in decibels L as a function of the root-mean-square (rms) reflector surface deviation δ and wavelength λ are given by

$$\eta_s = e^{-\left(\frac{4\pi\delta}{\lambda}\right)^2} , \tag{3}$$

$$L = 686\left(\frac{\delta}{\lambda}\right)^2 . \tag{4}$$

Figure 2 is a plot of the above relation, showing that a surface accuracy of 0.008 in results in a loss of about 0.6 dB at 44.5 GHz.

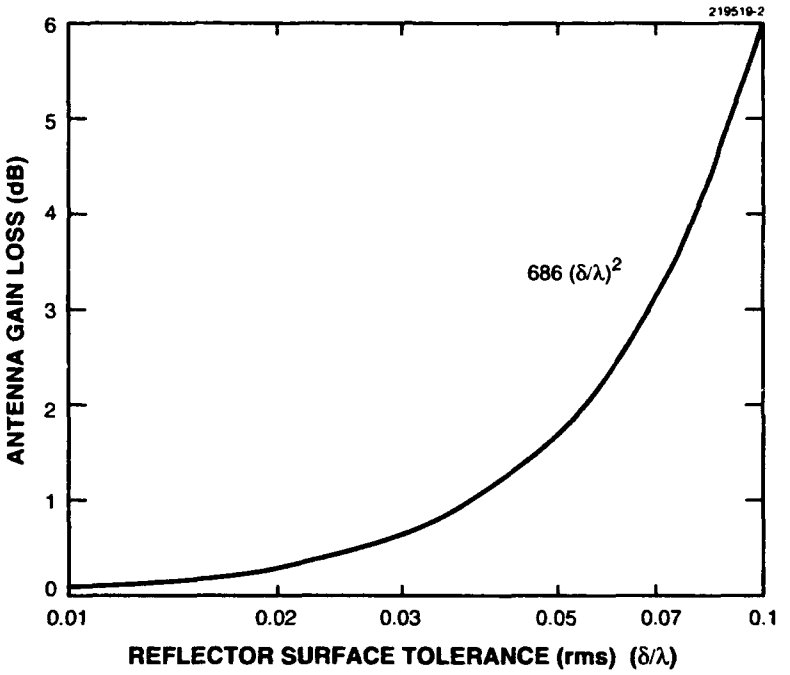

Figure 2. Antenna gain loss due to reflector surface tolerance.

Compared with other types, the reflector antenna could best meet ASCAMP requirements, and therefore, was selected. To maintain good surface accuracy and construction simplicity, a one-piece solid reflector was preferred. The high gain requirement, however, dictated a larger aperture than could be easily carried. As a result, unfurlable or deployable reflector possibilities were explored. Some options were an air-inflatable balloon, an unfurlable wire mesh, and deployable petal reflectors.

Air balloons were considered not rigid enough to maintain the proper reflector shape. A wire-mesh reflector, which deploys like an umbrella, has proven quite useful at UHF but unsuitable at EHF because of the surface accuracy requirement. Semirigid reflector petals assembled on a hub with latches and edge connectors were chosen for the deployable reflector design.

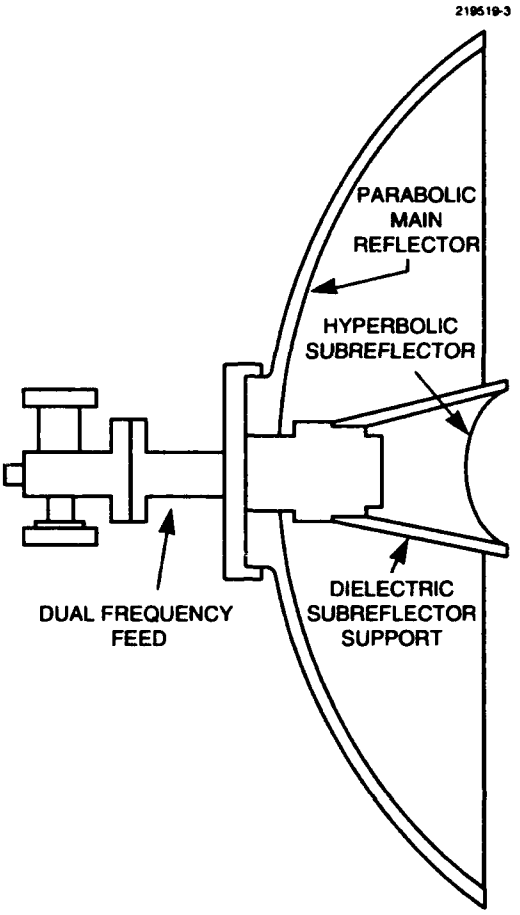

Figure 3. SCAMP dual-band antenna, Cassegrain design.

2.5 REFLECTOR GEOMETRY

Three reflector geometries were considered—Cassegrain, offset, and displaced axis.

2.5.1 Cassegrain Reflector

The original SCAMP system used a standard Cassegrain antenna design (Figure 3) that optimized Q-band performance and settled for resulting K-band performance. This flexibility was possible because the requirement for the antenna gain at K-band was rather undemanding, and no problem was encountered in meeting the system specification. This Cassegrain system consists of a 10-in parabolic main reflector ($F/D = 0.25$), a hyperbolic subreflector (eccentricity = 1.67), and a dual-band, modified SCOTT feed [3]. An electrically small ($D/\lambda \leq 10$) Cassegrain antenna creates conflicting design considerations between feed blockage and subreflector spillover losses, leading to low efficiency for all small Cassegrain antennas. Because the antenna gain requirement for both bands is greatly increased for ASCAMP, the Cassegrain reflector was not a good design candidate.

2.5.2 Offset Reflector

Another approach considered was an offset reflector utilizing a dual-frequency feed such as the unit originally designed for the SCOTT ADM. Advantages of this geometry are good demonstrated antenna performance in both bands with low sidelobes and no feed blockage loss. Disadvantages are that the reflector is asymmetric and each reflector petal is different; the reflector has an elliptical cross section with the longer reflector dimension about 20% longer than that of the projected aperture, thus making the reflector heavier than a non-offset design, and the asymmetry of the reflector results in some beam squint loss. These deficiencies make this approach less interesting.

2.5.3 Displaced Axis Reflector

The axis-displaced ellipse (ADE) antenna design is a centrally fed, displaced axis parabolic reflector with a dual-frequency ring-focus feed. The subreflector is a surface of a revolution of a section of a tilted ellipse.

The ADE antenna is inherently better matched and more uniformly illuminated than conventional centrally fed, parabolic reflector antennas and, therefore, is more efficient. Its main advantages are:

- Relatively high aperture efficiencies for main reflector diameters as small as 10 wavelengths
- Subreflectors several times smaller than those used in Cassegrain antennas
- Feed impedance mismatch and main reflector blockage minimized due to subreflector shape
- High aperture efficiency resulting from the ray inversion feature of the elliptical subreflector, making the final illumination of the main reflector more uniform.

For compactness and good electrical performance, the centrally fed, displaced-axis ADE antenna was chosen for use with ASCAMP.

3. ASCAMP ANTENNA ELECTRICAL DESIGN

The single-band ADE antenna was invented by J.L. Lee in 1964 [4] and extensively investigated in the (former) Sovet Union [5–7]. Lincoln Laboratory developed dual-band EHF ADE antennas of 6- and 12-in diameters. Their measured efficiencies were 43% and 52%, respectively, in the low-frequency band and 62% to 63% in the high-frequency band [8].

3.1 DESIGN EQUATIONS

Figure 4 is a schematic diagram of an ADE antenna. A list of symbols used in the figure and the design equations follows.

F = focal length of main reflector
f = minimum distance of subreflector ellipse to focus
y = perpendicular distance of main reflector from A-A
D = diameter of main reflector
d_s = focus ring diameter of subreflector
d_m = axis displacement of main reflector
O = feed phase center; focus no. 2 of ellipse
T = tip of subreflector
L = distance from O to T
Q = outer edge of main reflector
F_r = ring-focus location; focus no. 1 of ellipse
A-A' = symmetry axis of rotation
B-B' = displaced axis; axis of parabola
B-F_r = focal length of parabola
ε = eccentricity of ellipse; <1
ϕ = angle of O originated ray from A-A
ψ = angle B-F_r-Q
φ_1 = ellipse major axis tilt angle from A-A
ψ_0 = angle O-F-Q
ρ = subreflector polar distance from O.

The five design equations are:

$$\varepsilon = \frac{\sin\frac{\psi_o}{2}}{\sin\left(\frac{\psi_o}{2}+\phi_1\right)} \quad , \tag{5}$$

$$f = \frac{d_s \cos\frac{\psi_o+\phi_1}{2}}{4 \sin\frac{\psi_o}{2} \cos\frac{\varphi_1}{2}} \quad , \tag{6}$$

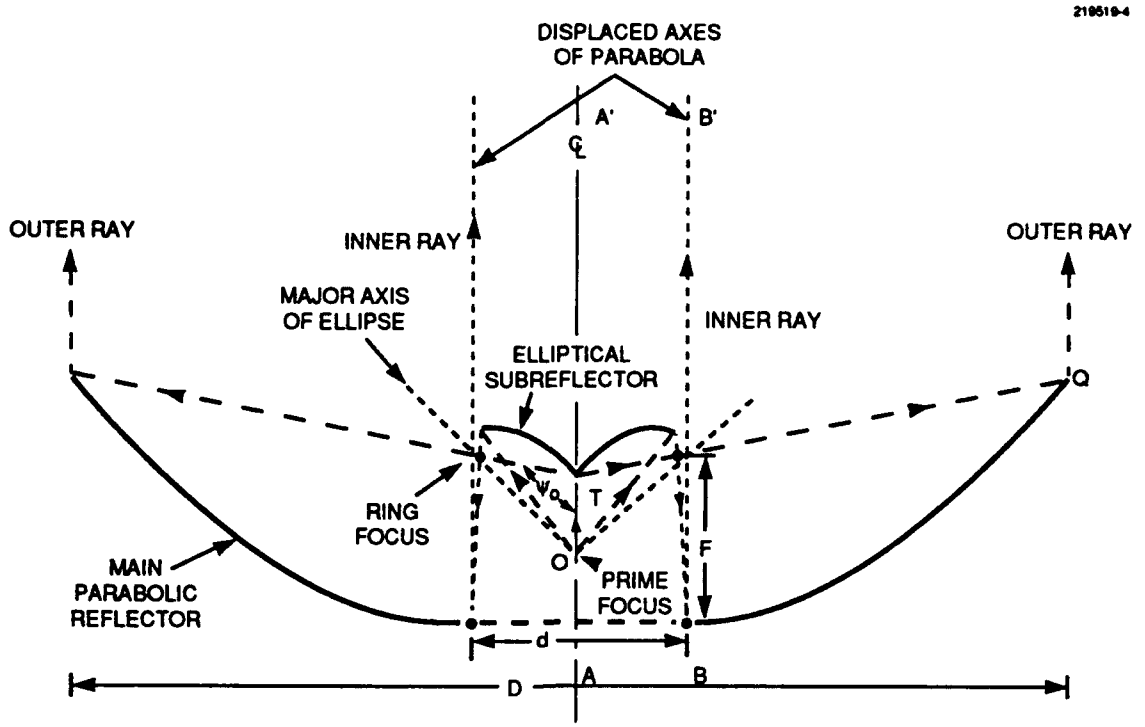

Figure 4. Geometry of an ADE antenna.

$$\rho = \frac{(1+\varepsilon)\ f}{1-\varepsilon\ \cos\left(\varphi_1 - \varphi\right)} \quad , \tag{7}$$

$$y = 2F\ \tan\frac{\varphi}{2} + \frac{d_m}{2} \quad , \tag{8}$$

$$L = \frac{d_s}{2}\left(\cot\ \varphi_1 + \cot\ \psi_o\right) \quad . \tag{9}$$

Given φ_1, Ψ_o, and d_s, then f, ε, and ρ can be calculated from Equations (5), (6), and (7). With $y = D/2$ and $\psi = \psi_o$, F can be calculated from Equation (8). Equations (7) and (8) determine the contours of the sub- and main reflector surfaces, respectively. Equation (9) fixes the relative locations of the feed and subreflector. The relative locations of the main- and subreflectors are fixed by the "coincidence" of the two focus rings.

Based on geometric optics, the original ADE design used $d_s = d_m$, or the ratio $d_s/d_m = 1$. It was found experimentally that by making the ratio slightly larger than 1, the ADE antenna gain can be further improved [6]. A ratio of 1.035 was used for ASCAMP. Equations (5), (6), and (9) result in $L = 1.974$ in, $f = 0.494$ in, and $\varepsilon = 0.738$ with $\phi_1 = 40$ deg, $\psi_o = 95$ deg, and $d_s = 3.576$ in. Using Equation (8), $F = 4.707$ in with $D = 24$ in. Figure 5 is a drawing of the antenna with feed.

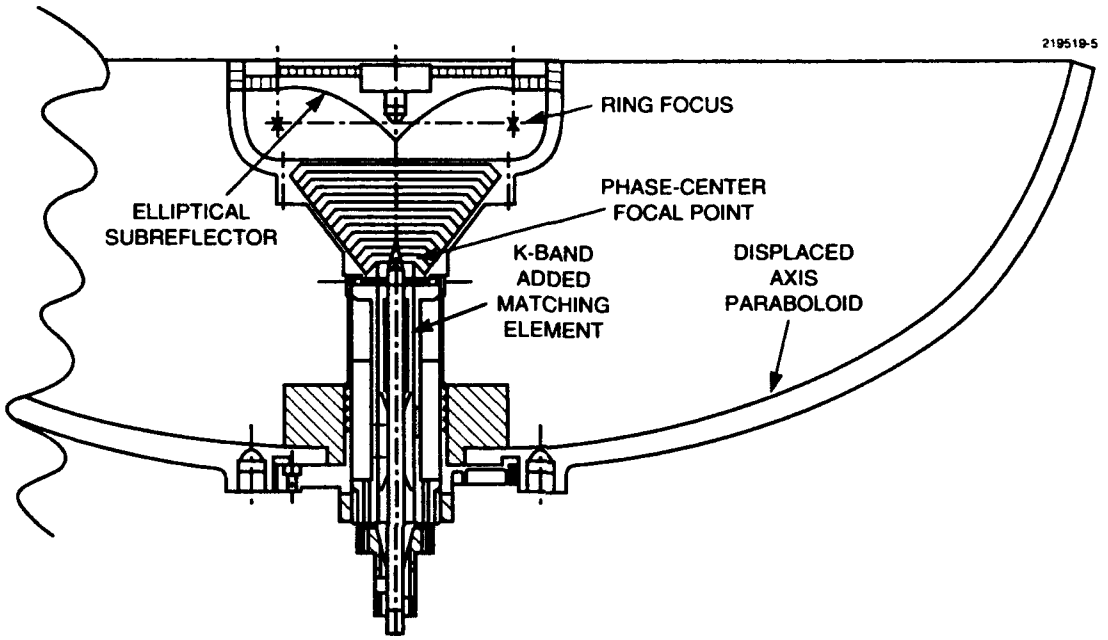

Figure 5. ASCAMP antenna design.

4. RING-FOCUS FEED

When the elliptical subreflector is considered as part of the feed, the feed phase center forms a ring. Without the subreflector this feed is very similar to that of the SCOTT ADM [3]. As described next, some changes and improvements were made to optimize ASCAMP antenna performance and to minimize weight.

The basic structure of the feed consists of two concentric circular cylinders that form a coaxial structure. The outer coaxial waveguide is used for the low-frequency band, and the inner circular waveguide is for the high-frequency band.

4.1 FEED REQUIREMENTS

The two bands of interest are K (20.2 to 21.2 GHz) and Q (43.5 to 45.5 GHz). General requirements for the feed are compact size, lightweight, rugged construction, and easy fabrication. The RF performance requirements are

- Symmetric feed radiation amplitude pattern with suitable taper (about 15 dB) for efficient illumination of the subreflector in both bands
- Coinciding phase centers for both bands
- Circular polarization with a small axial ratio in both bands
- Low VSWR and transmission losses
- High isolation between the two frequency bands.

4.2 FEED DESIGN

A blowup of the feed design is given in Figure 6. The total subtended angle of the corrugated horn is 80 deg. The core of the feed is a compactly designed dual-band rectangular-to-coaxial circular waveguide junction [9]. There are two signal paths—the Q-band 44-GHz uplink and the K-band 20-GHz downlink.

Mechanical designs of the key components of the feed are kept simple. Additional components such as input/output waveguide ports, polarizers, terminations, etc. are fitted along with specially designed matching elements. To save space, unwanted cross-polarized signals in both bands were terminated using internal loads. Some components are multifunctional and used whenever possible as follows:

- Corrugated horn, which shapes the primary pattern for both bands
- K-band rectangular-to-circular coaxial waveguide junction, which plays the triple role of 90-deg bend, mode transducer, and impedance transformer
- Corresponding Q-band junction, which plays a similar triple role
- K-band impedance matching ring, which also works as an alignment spacer

- Q-band dielectric polarizer/wave-launcher, which is one machined piece
- Axial holes, which reduce the effective dielectric constant in the Q-band wave-launcher also serve as vent holes for dry air purging
- Dual-band radome covering the horn opening, which also holds the subreflector.

For the best illumination efficiency in both bands, a wide flare-angle corrugated horn producing a spherical wave front is used. Under this condition, the primary pattern is not frequency sensitive but is controlled mainly by the flare angle. This design has low loss (as was demonstrated in SCOTT). When this feed was used with a solid offset reflector with a 24-in-diameter circular aperture, an overall antenna efficiency (including feed loss) of over 60% compared with lossless uniform illumination was obtained for both bands.

For ASCAMP, the bandwidth of the feed impedance match was increased for the K-band coaxial waveguide opening by adding another matching element. The matching bandwidth for the Q-band junction was also improved by shaping the septum at the junction. A metal ridge polarizer attached only to the K-band outer wall of the coaxial waveguide was used instead of the original dielectric slab design.

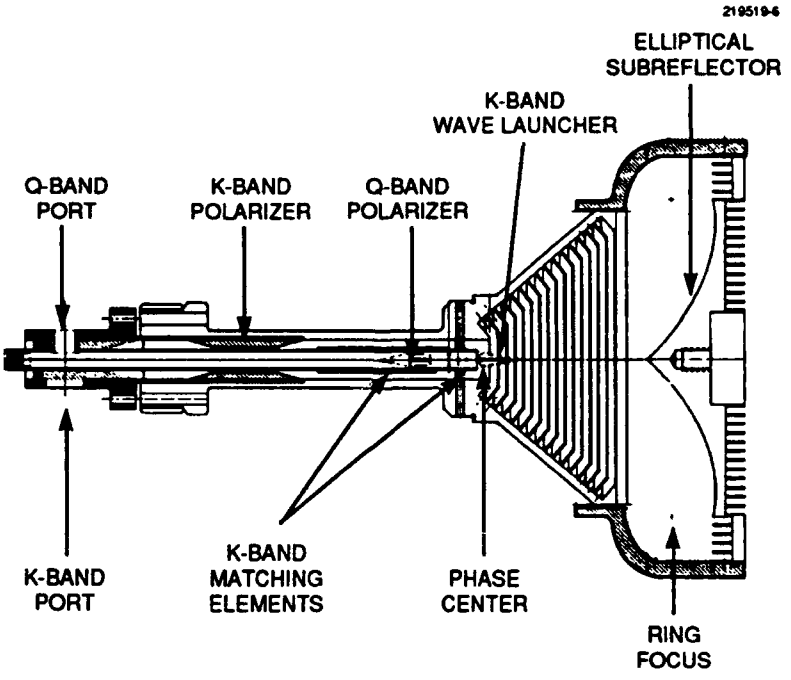

Figure 6. Blowup of ASCAMP antenna feed.

The Q-band wave-launcher/polarizer is made of a single piece of Rexolite. This change avoided the rather inexact gluing process between the Teflon wave-launcher and the Rexolite polarizer plate used in the original SCOTT design. Four longitudinal holes were placed in the new wave-launcher to reduce its effective dielectric constant, which is necessary to control higher-order modes. The horn polarization sense for both bands was changed to accommodate the additional reflection from the subreflector. Compared to the 6- and 12-in ADE antennas developed earlier, the current larger (24-in) reflector relieved some constraints on feed and subreflector size. For high efficiency, the feed horn was enlarged and corrugated. The added length to the feed permitted the use of an additional K-band matching element to improve the impedance match at the coaxial waveguide opening. The corrugations on the subreflector act to reduce stray currents at the edge and back of the subreflector.

The K- and Q-bands feed performance is shown in Figures 7 and 8, respectively. The return losses of about 20 dB were obtained for each section of the signal path in both frequency bands of interest, guaranteeing good overall impedance match with negligible mismatch loss. The low axial ratio (below 1 dB for both bands) guarantees good circular polarization. Clean radiation patterns are hard to measure with the subreflector due to unavoidable scattering off the connecting waveguide. Figures 9 and 10 give the feed radiation patterns without the subreflector in Q- and K-bands, respectively. As can be seen, the

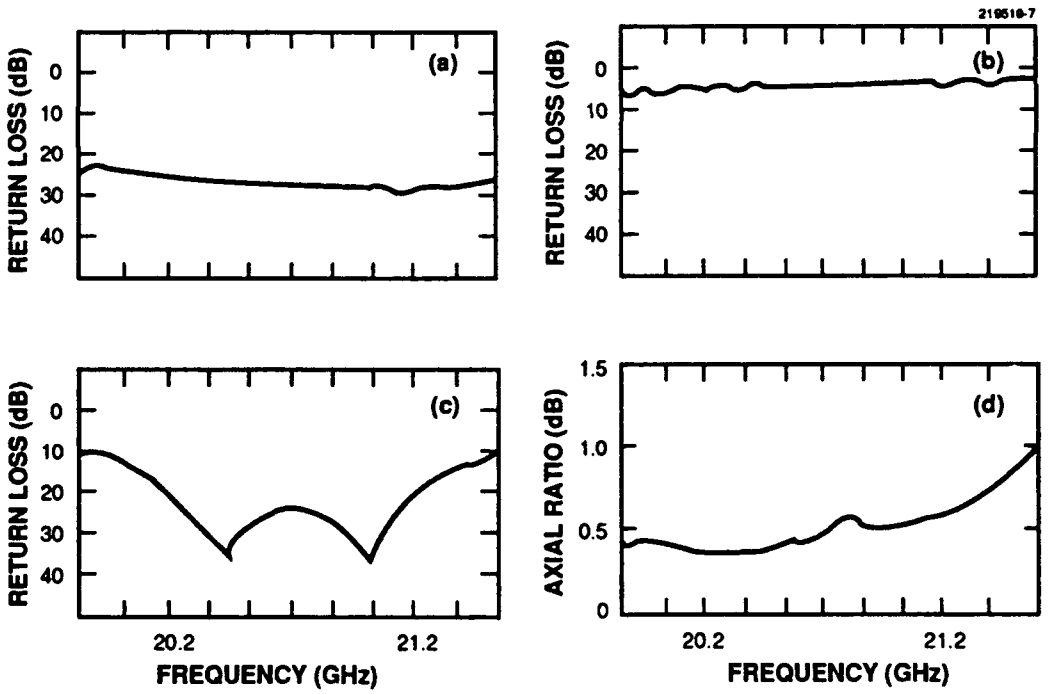

Figure 7. Feed performance, K-band. Match (a) of orthomode transducer, (b) without tuning ring, (c) at waveguide input without polarizer, and (d) axial ratio of polarizer.

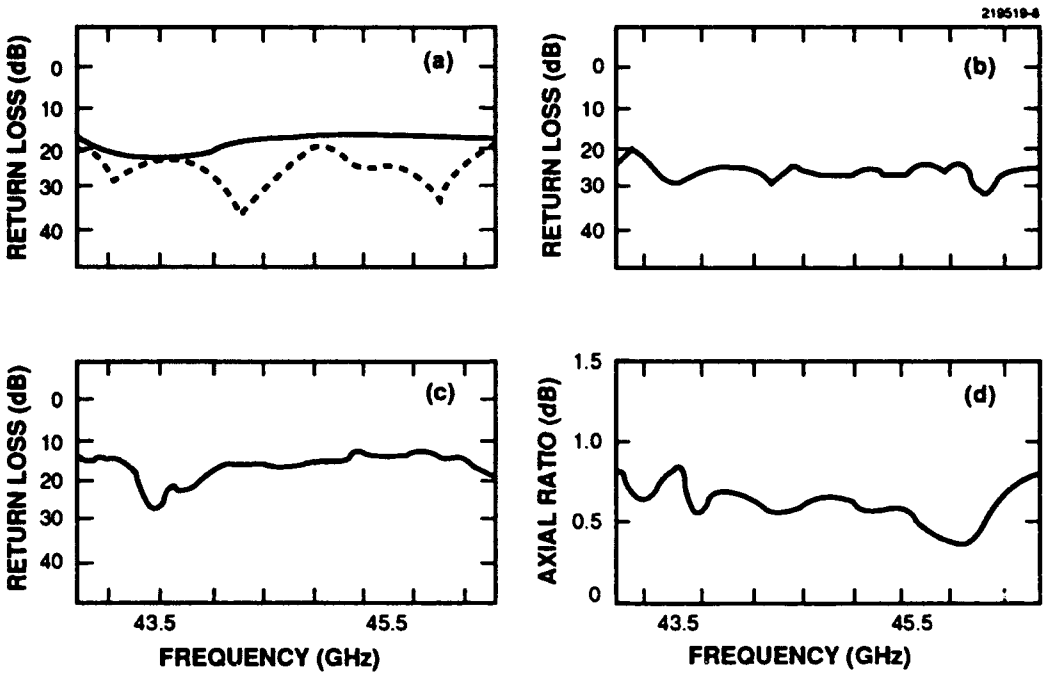

Figure 8. Feed performance, Q-band. (a) Match at the orthomode junction, (b) isolation measured between K- and Q-ports, (c) match of short load, and (d) axial ratio.

required 15-dB amplitude tapers for both bands at about a 40-deg angle were realized. In these measurements, rotating linearly polarized transmitting antennas were used to show the feed polarization characteristics. The measured small excursions in pattern response level showed that the feed was circularly polarized with good axial ratios in both bands.

The dual-band radome/subreflector holder used a partial toroidal surface with the focus ring as its center. Several dielectrics such as Teflon, polyethylene, Plexiglas, Rexolite, and Rohacell rigid foams were considered as the radome material. Rexolite was chosen for its rigid mechanical strength and low-loss dielectric property. The thickness of the RF-active region was chosen to be one wavelength at 44.5 GHz. Because this length is close to half wavelength in the 20.2- to 21.2-GHz band, good impedance matches were obtained in both bands.

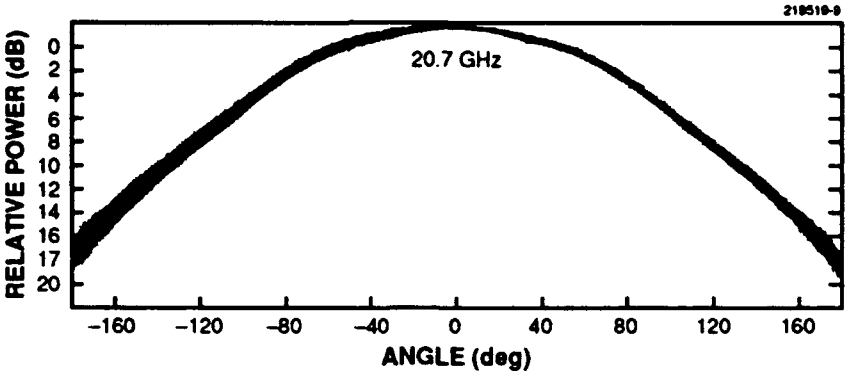

Figure 9. Feed pattern without subreflector, K-band

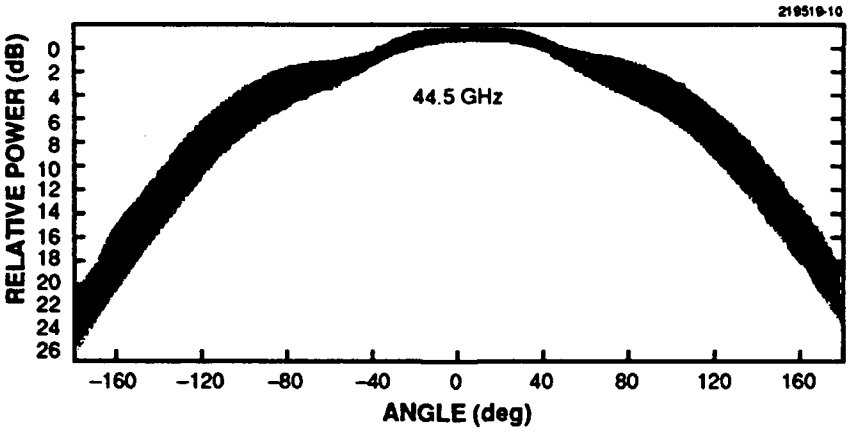

Figure 10. Feed pattern without subreflector, Q-band.

5. REFLECTOR DESIGN AND FABRICATION

The reflector (d_m = 1.728 in, F = 4.707 in, D = 24 in) was purchased from a vendor on a best-effort basis. The reflective surfaces of the petals are made of 3-mil aluminum foil molded with graphite/epoxy backed with lightweight honeycomb core construction of about 0.25-in thickness. The weight is 2.6 lb, including a hub and six petals. Each petal weighs about 6 oz and is made from a precise mold with a measured surface tolerance of 0.003 rms. Assembled, the six petals are pinned and locked with a locking nut to a central hub and to each other at their outer radial edges with a pin/spring latch. The retaining force of the latch is 0.4 lb. The spring constant was 5 lb/in. Figure 11 details the mounting interfaces of the reflector petals and the central hub.

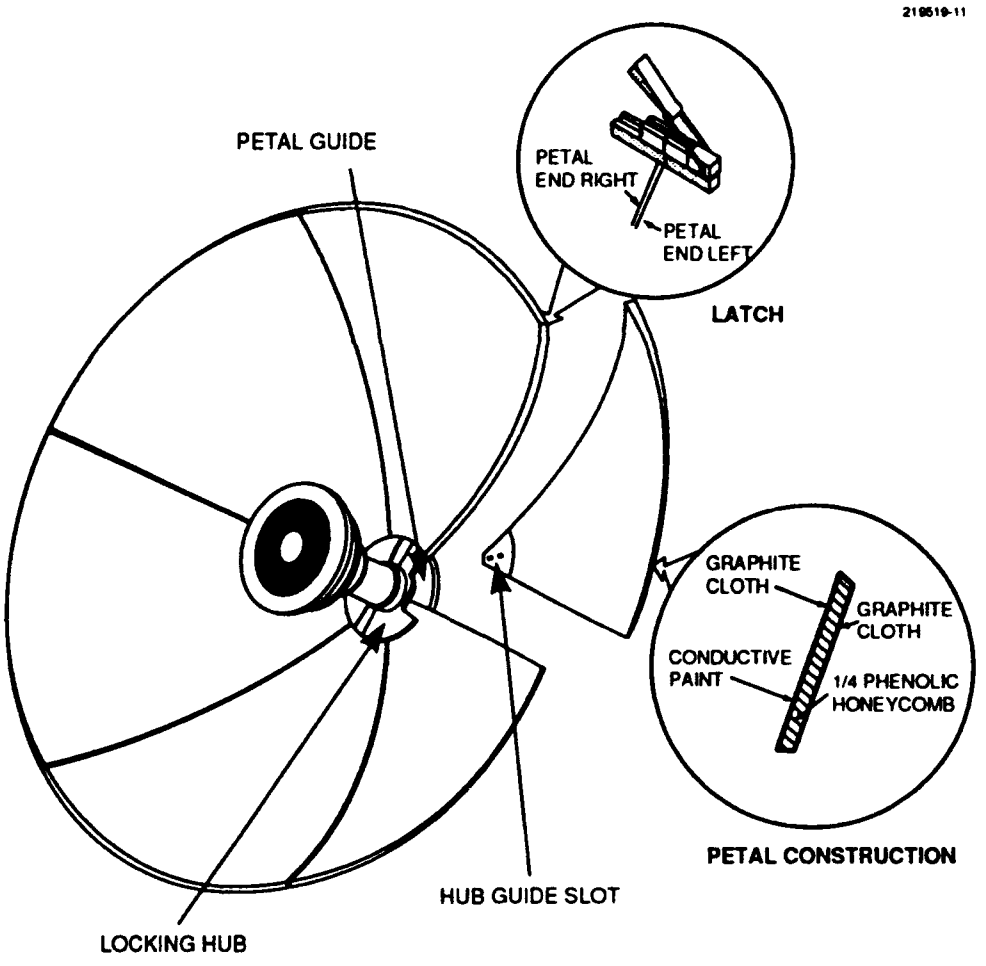

Figure 11. Deployable petal antenna design concept.

6. ANTENNA PERFORMANCE

6.1 MECHANICAL

The center-fed antenna design is physically symmetric and thus most efficiently uses the reflector surface. The surface tolerance goal, including assembly misalignment of the assembled reflector, was 0.008-in rms. Losses of 0.2 and 1 dB were expected in the lower and higher bands, respectively, due to misalignment of the reflector petals.

Measured surface contours of the first manufactured deployable antenna are plotted in Figure 12, which indicates a peak variation of about ± 0.040 in. The corresponding rms value is 0.016 in. If this were truly a random surface variation, the loss in antenna gain would be 2.6 dB at 44.5 GHz. When the

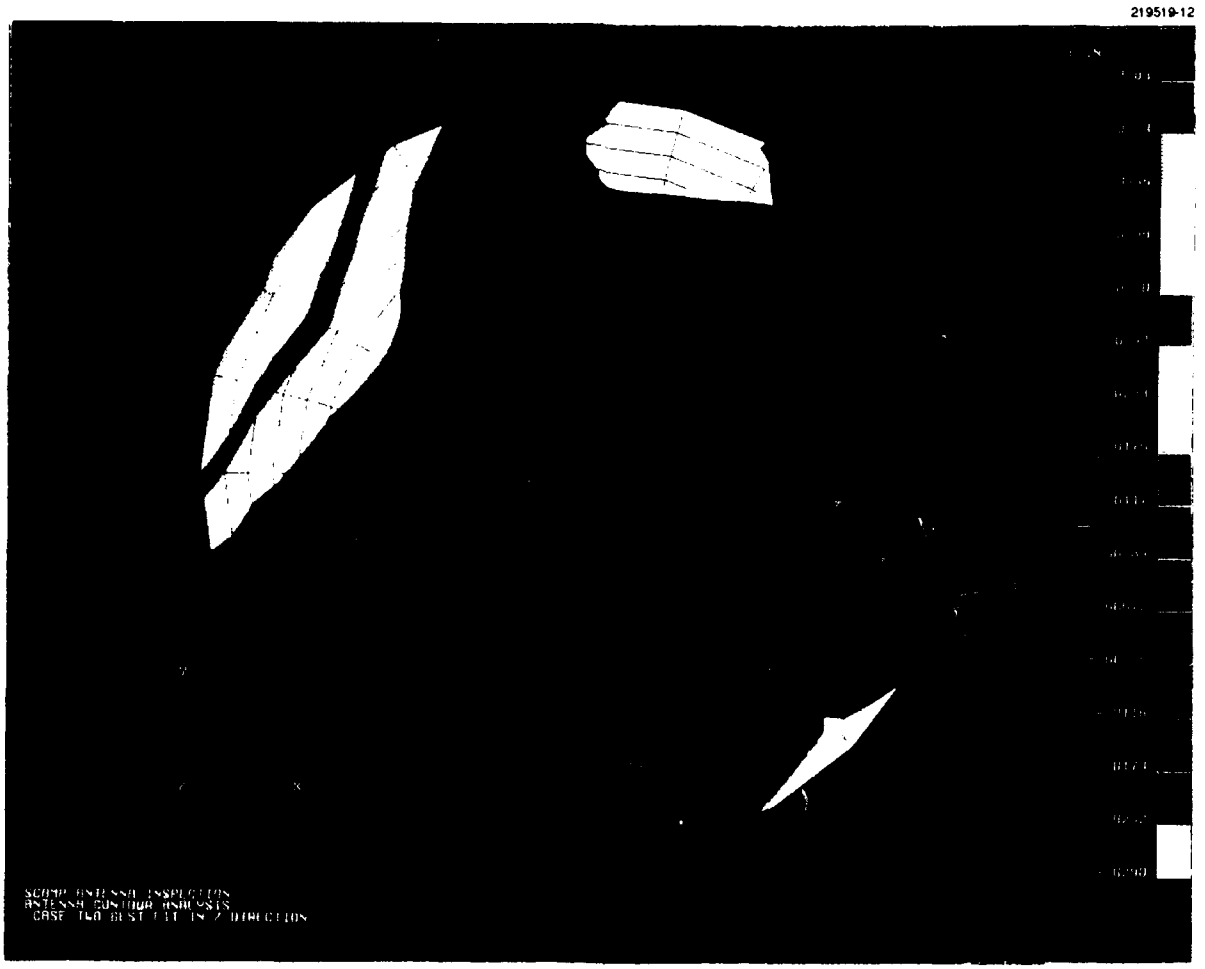

Figure 12. Petal antenna surface contour plot.

deviations were corrected for best fit to an ideal displaced axis parabola, the effective surface accuracy dropped to about 0.010-in rms. Antenna gain loss for this surface accuracy is about 0.95 dB. By actual electrical measurements, the loss of antenna gain due to petal misalignment was less than half the calculated loss using the mechanically measured overall rms values. The macroeffects of Petal misalignment seem less important than the microeffects of real surface roughness. In general, the fact that in most antenna systems the feed location has a looser tolerance than the required surface tolerance seems to reinforce this reasoning.

6.2 ELECTRICAL

For reference purposes, measurements were made using a precisely machined solid aluminum reflector. Figures 13 and 14 are pictures of the solid and Petal reflector antennas. The final feed and subreflector axial locations were fine-tuned to maximize the Q-band gain. Antenna gains and patterns were first measured in an open field ground reflection range. Later the same measurements were repeated in a compact range. Antenna gain was measured by comparison with two 24-in, single-band, primary feed reflector antennas, one for each band. Each reflector antenna was carefully calibrated against a standard gain horn.

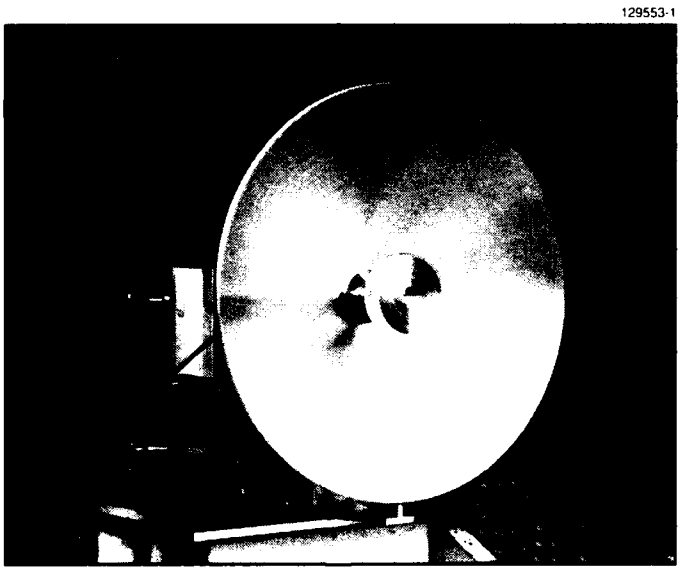

Figure 13. ASCAMP antenna, solid reflector.

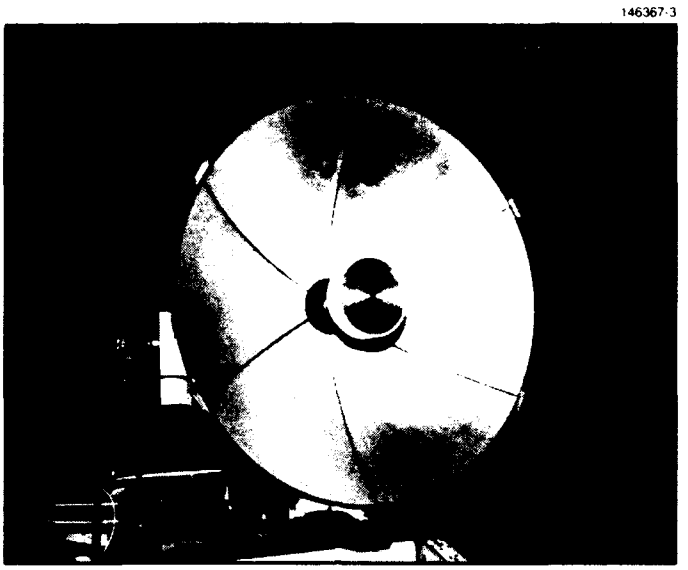

Figure 14. ASCAMP antenna, petal reflector.

Frequency was automatically swept in 0.1-GHz steps at both the Q- and K-bands. To increase accuracy during the open field measurements, all swept gain measurements were repeated four times in each band. No averaging was needed during compact range measurements because the system was very stable. Results obtained from the two measurements were within the measurement error of about 1 dB. Compact range swept gain measurements for both the solid and petal reflectors in the Q- and K-bands are given in Figures 15 and 16. The antenna gains at the center and end frequencies with solid and Petal reflectors and other related parameters are given in Table 1.

Using a solid aluminum reflector, the average efficiencies for the whole up- and downlink bands are 69% and 56%, respectively. The petal reflector has corresponding efficiencies of 65% and 55%, an average gain reduction of only 0.29 and 0.08 dB, respectively, due to Petal assembly surface imperfections.

Radiation patterns were measured at the center and the two band-end frequencies. As expected, very similar patterns were obtained within each band. Only the patterns for each band center frequency are presented here. The measured wide-angle (−180 to +180 deg) radiation patterns for the solid and petal reflectors in the transmit and receive center frequencies are given in Figures 17 through 20. Blue and red

stand for elevation and azimuth cuts, respectively. Wide-angle patterns are useful for far sidelobe characterization. Note that there is some increase in far sidelobe levels for the Petal reflector. The backlobe level was limited by system noise. By reducing the receiver bandwidth to 3.2 Hz and employing over 2,000 samples averaging, the system noise level was effectively reduced. Under this condition a "cleaner pattern" is shown in Figure 21. The generally low level of the far-out sidelobes, approximately 80 dB down, indicates that the terminal has a very low probability of intercept. It should be emphasized that the final far sidelobe levels are expected to be sensitive to the details of the antenna installation environment.

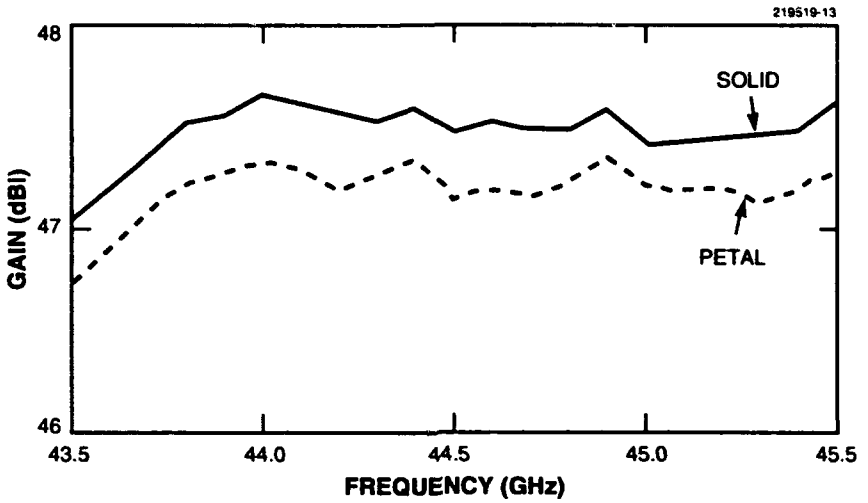

REFLECTOR	G_{ave} (dBI)	EFFICIENCY (%)	STANDARD DEVIATION (%)	G_{max} (dBI)	G_{min} (dBI)
SOLID	47.47	69	3	47.64	47.05
PETAL	47.18	65	3	47.34	46.74

Figure 15. Q-band swept frequency gain measurement

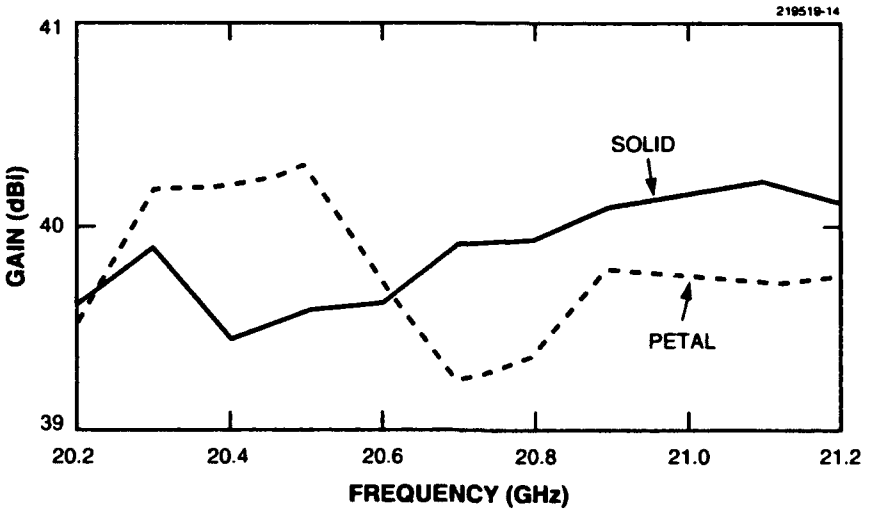

REFLECTOR	G_{ave} (dBi)	EFFICIENCY (%)	STANDARD DEVIATION (%)	G_{max} (dBi)	G_{min} (dBi)
SOLID	39.90	56	6	40.25	39.46
PETAL	39.82	55	7	40.30	39.27

Figure 16. K-band swept frequency gain measurement.

TABLE 1

Antenna Gain

Frequency (GHz)	Solid Gain (dBi)	Petal Gain (dBi)	Gain Loss (dB)	Average Antenna Efficiency	
				Solid	Petal
43.5	47.05	46.74	0.31		
44.5	47.46	47.15	0.31	69%	65%
45.5	47.62	47.28	0.34		
20.2	39.60	39.54	0.06		
20.7	39.93	39.27	0.66	56%	55%
21.2	40.15	39.78	0.37		

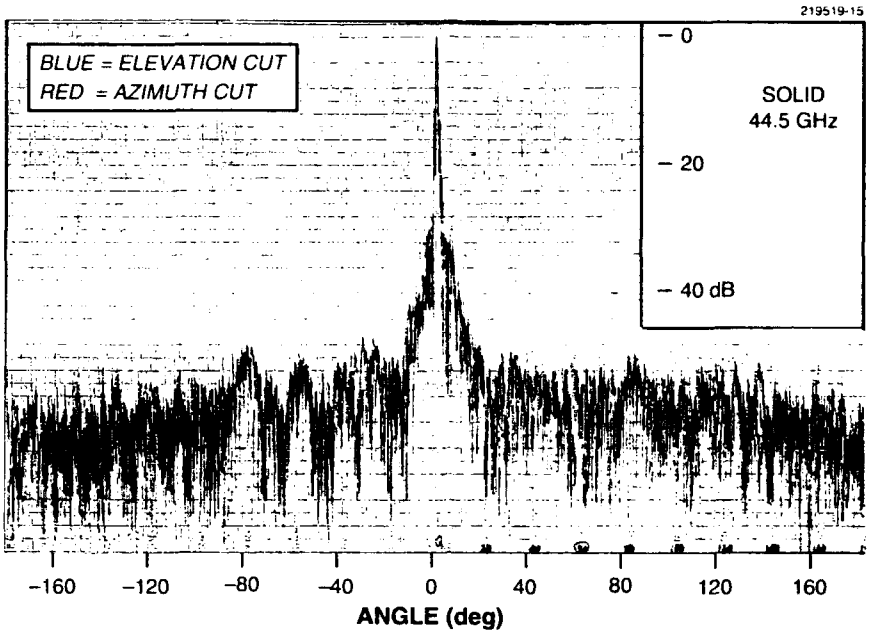

Figure 17. Wide-angle radiation pattern, solid reflector, Q-band.

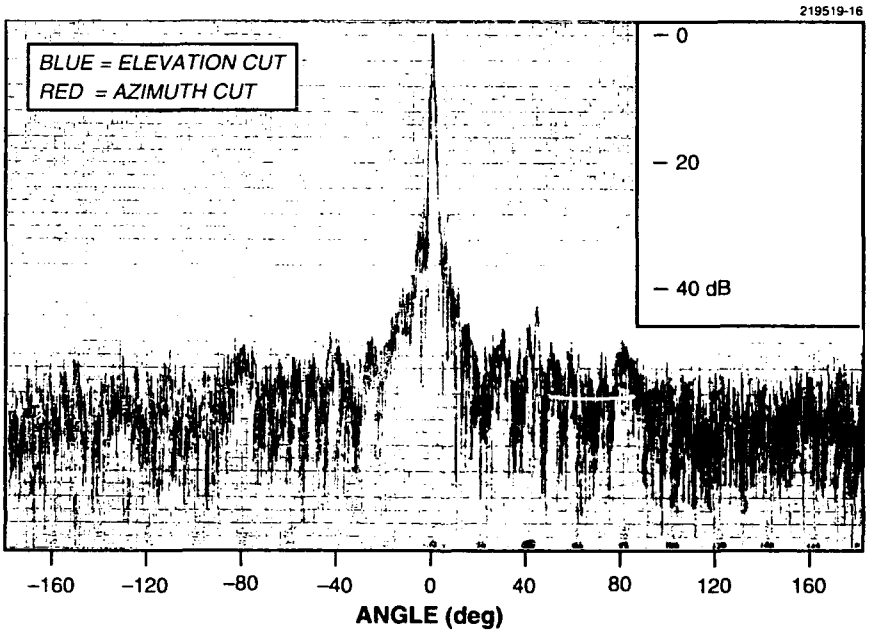

Figure 18. Wide-angle radiation pattern, Petal reflector, Q-band.

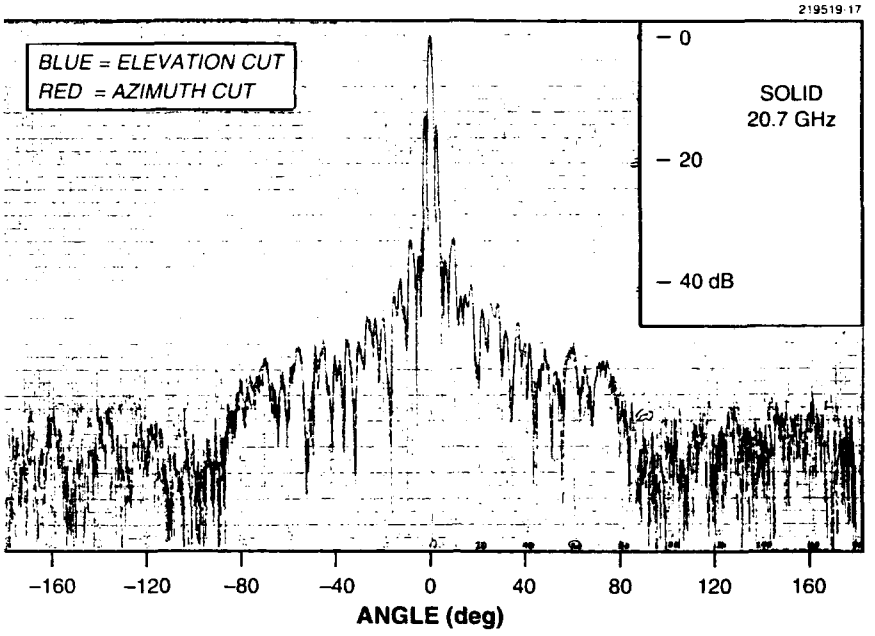

Figure 19. Wide-angle radiation pattern, solid reflector, K-band.

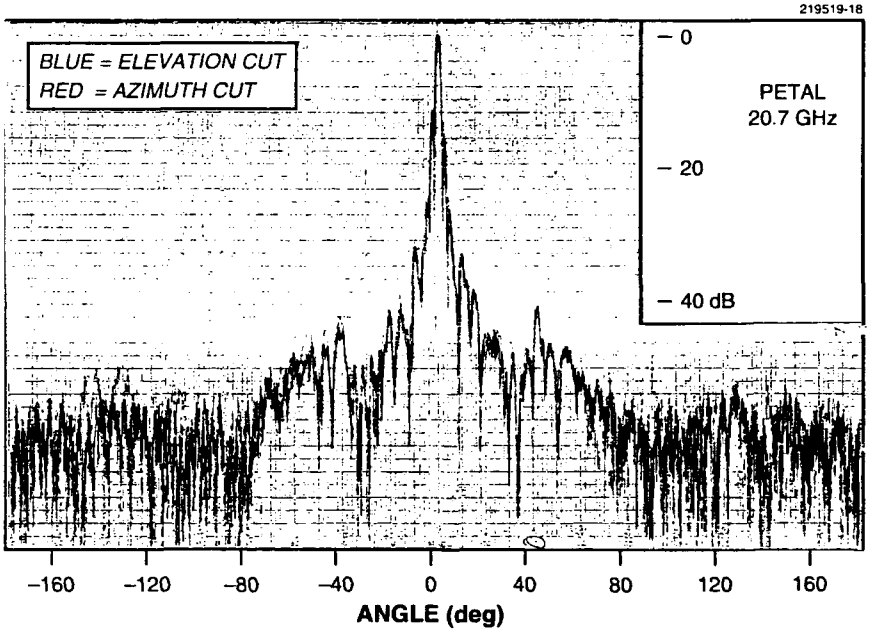

Figure 20. Wide-angle radiation pattern, Petal reflector, K-band.

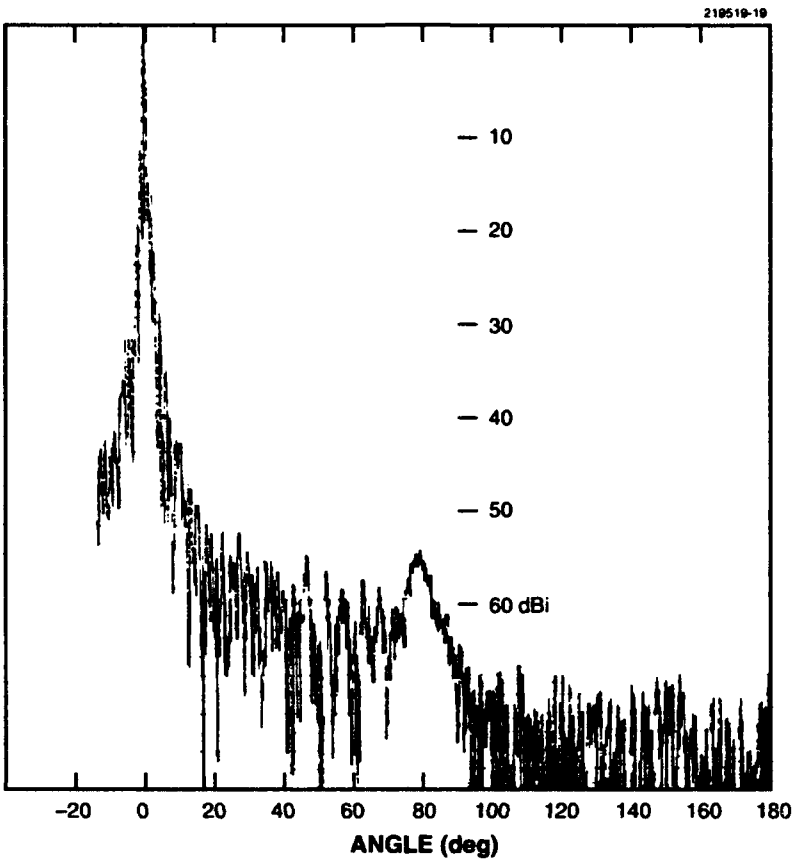

Figure 21. Backlobes radiation pattern, petal reflector, Q-band.

Corresponding close-up patterns useful for main beam and close-in sidelobe characterization are given in Figures 22 through 25. The relatively high first sidelobe (about –14 dB), characteristic of ADE designs, is due to the unilluminated center aperture area. Note that high close-in sidelobes are also consistent with high aperture efficiency. This definite feature of high first sidelobes in the receive frequency band can be used to advantage to facilitate satellite acquisition [10].

To check the repeatability of the petal shape, the antenna was recurrently assembled and disassembled in various orders. At each assembly the swept frequency measurements of antenna gain were made at Q-band. The repeated antenna gain measurements did show some statistical variations; however, no significant antenna gain difference due to different petal order was observed. Figure 26 shows the results of 10 trials. The maximum peak-to-peak gain excursion is about 0.4 dB. Thus the petal has good performance repeatability.

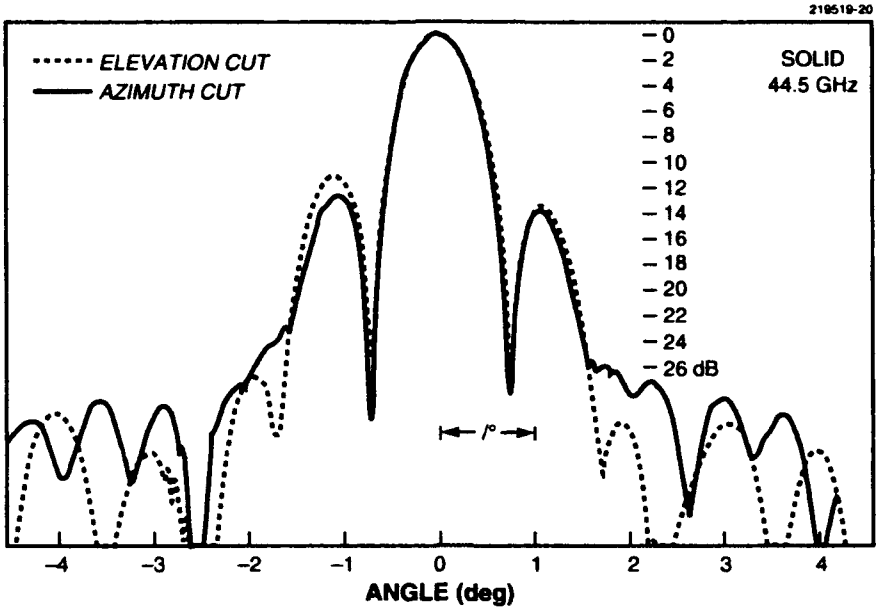

Figure 22. Close-up radiation pattern, solid reflector, Q-band.

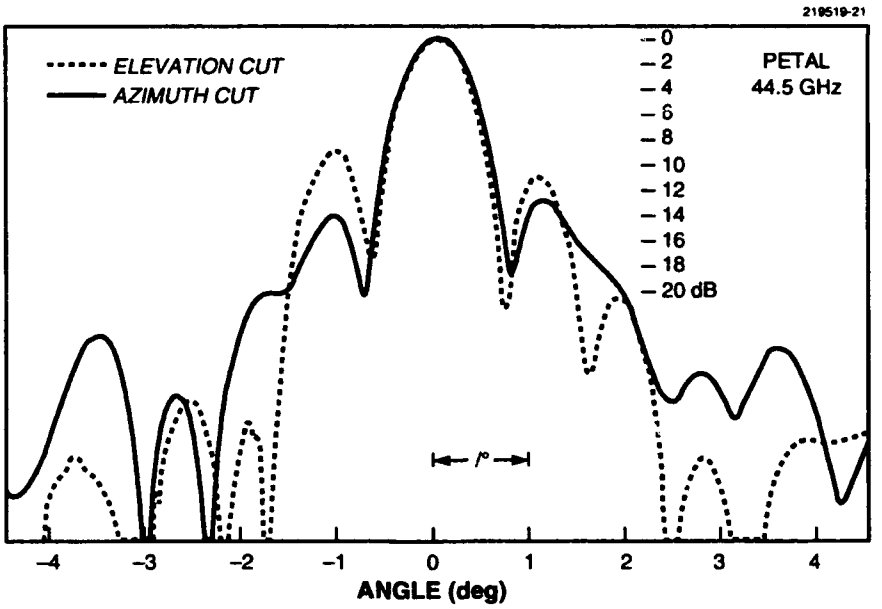

Figure 23. Close-up radiation pattern, petal reflector, Q-band.

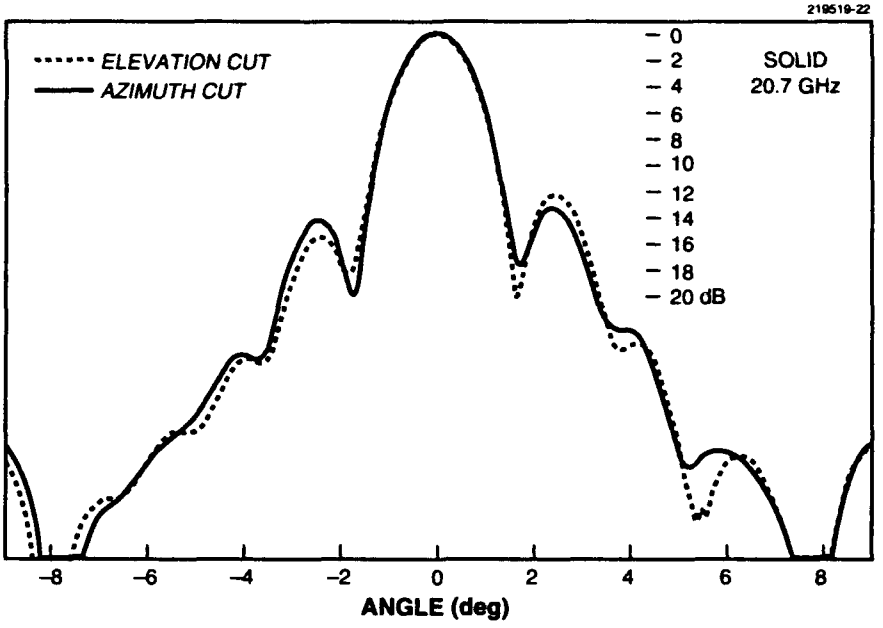

Figure 24. Close-up radiation pattern, solid reflector, K-band.

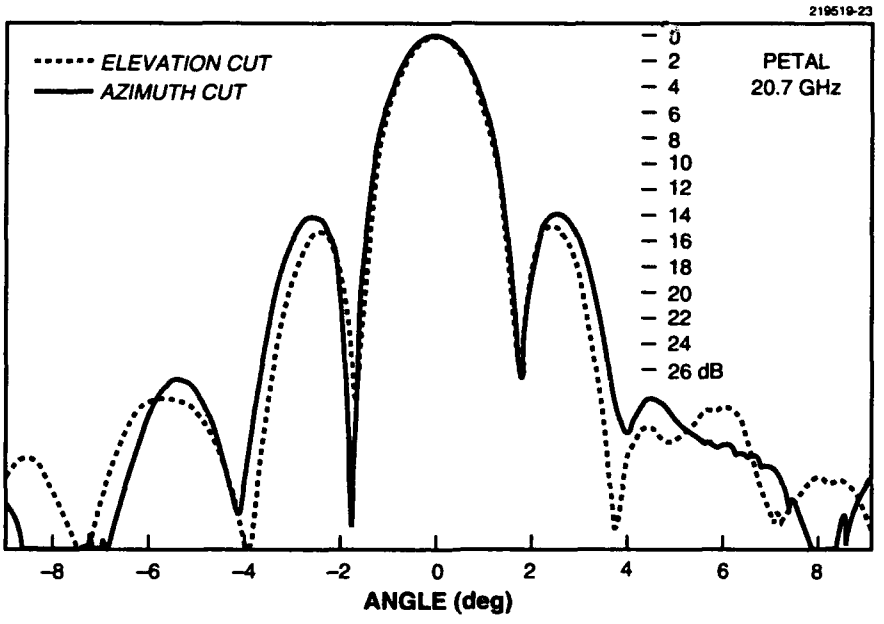

Figure 25. Close-up radiation pattern, petal reflector, K-band.

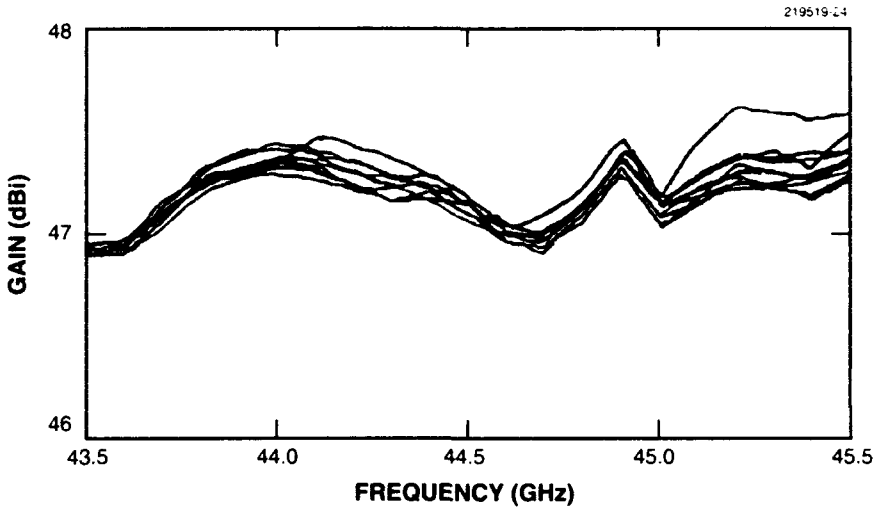

Figure 26. petal antenna repeatability test.

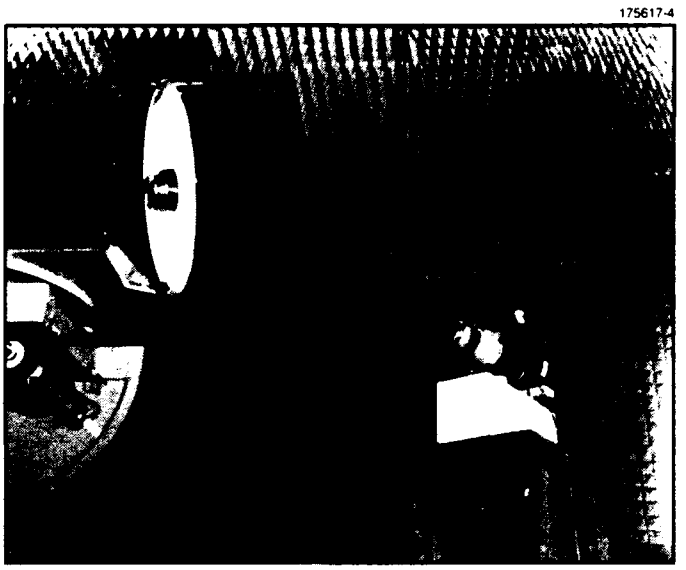

Figure 27. petal antenna under wind test.

To determine the effect of strong winds on the petal antenna, a 42-mph wind was generated by an 8-in blower (Coppus Vano 175). Figure 27 shows the test setup. The wind had no significant effect on the swept antenna gain, measured in the 42- to 46-GHz band.

The antenna was also tested for any squint between the two beams in the two bands by measuring and displaying two antenna patterns (one for each band) simultaneously and recording both on a dual-trace paper. The recorded patterns showed no measurable beam squint.

7. MECHANICAL CONSIDERATIONS

The Advanced SCAMP antenna reflector consists of six graphite-epoxy clad petals with phenolic honeycomb cores and conductive parabolic surfaces (Figure 28). Latch and striker devices embedded in opposing outer corners provide the necessary rim restraint. A threaded, flanged tube and oversized clamping nut combination serve as the central anchor of the antenna assembly. This tubular hub is also the feature used to mount and position the feed assembly. The clamping nut secures the tips of the petals.

7.1 PETAL REFLECTOR

The earliest petals were produced by first stretching a thin aluminum foil across a mold mixture followed by graphite and honeycomb layers. After curing and final finishing, the petals were examined for dimensional accuracy. Measurements revealed small but bothersome distortions of the petal reflecting surfaces. This warpage was attributed to the foil layer spring-back after the petals were removed from the mold.

Subsequent petals were fabricated, omitting the foil layer. The reflective surface was developed through a sprayed coating of silver epoxy paint. This secondary operation eliminated the stress-related distortions and created a highly conductive antenna facing at reduced cost.

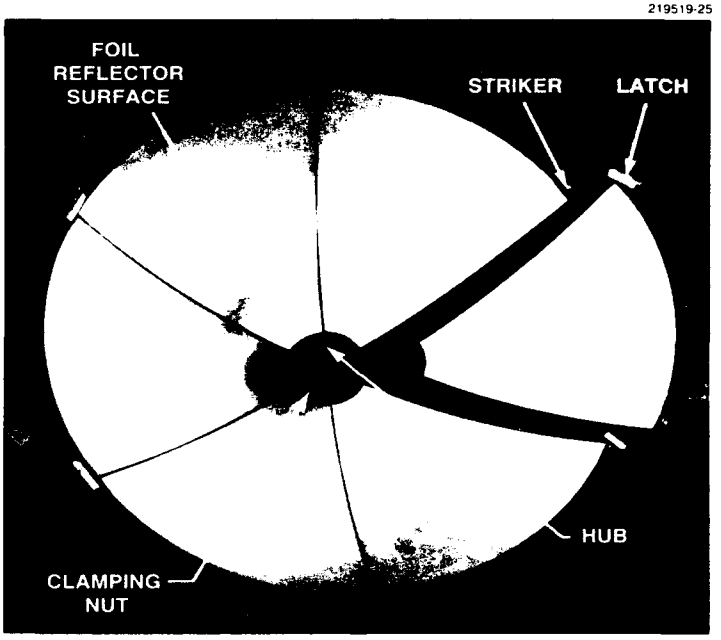

Figure 28. ASCAMP reflector components.

Petal edge restraints incorporated in the first petal set were over center-type clamping devices. These custom-designed miniature units also employed a retracting alignment pin housed in the striker assembly. Adjustment of these latches proved critical and inexact, resulting in noninterchangeable petal sets. Additional objections to this device were its complex actuation process and overall weight considerations.

7.2 CLAMPING DEVICES

A revised version of the original latch was fabricated using a spring-loaded clamp pawl. Introducing the spring eliminated any adjustment problems; however, the device remained bulky and awkward to use. It became clear that a more user-friendly, low-weight device was needed.

The redesigned latch assembly resembled a miniature elastic draw latch. Two extension springs, anchored at one end to a pivot pin that is located in one petal corner with the remaining ends looped around a second pin installed in a grip tab lever, define the latching mechanism (Figure 29). Embedded in the opposing corner of each petal is a hook-shaped keeper and a spring-retracted alignment pin (Figure 30). The final version uses a fixed pin, further reducing the cost and weight of this mechanism (Figure 31). This configuration produced a low-weight, single-action latch, which appeared to eliminate the drawbacks associated with the previous devices.

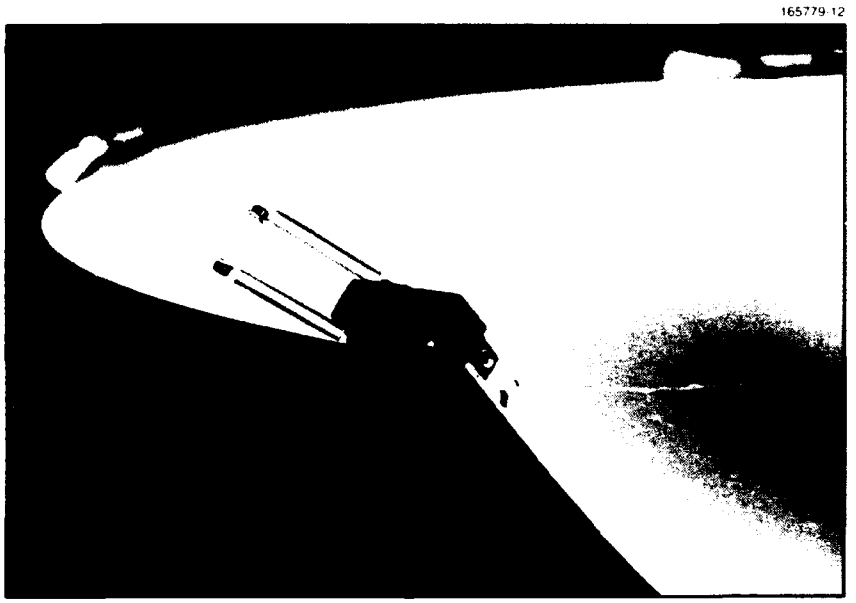

Figure 29. Reflector petal latch.

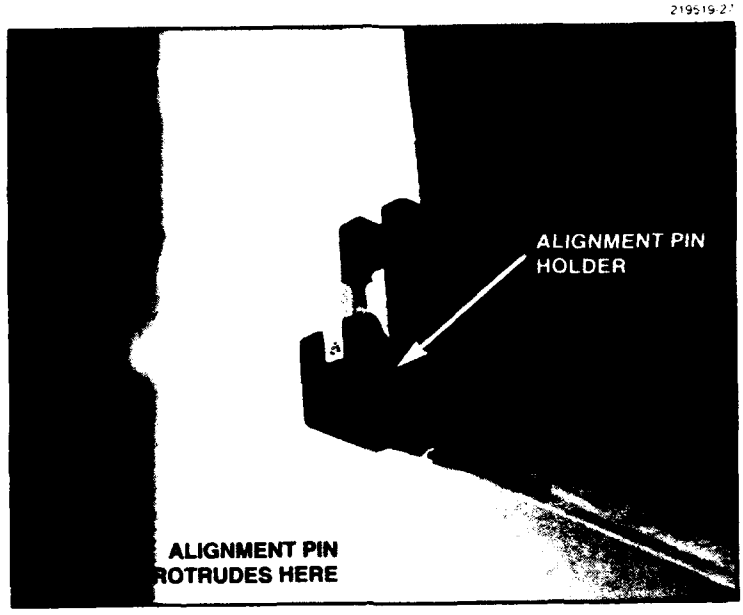

Figure 30. Reflector petal keeper, retracting pin.

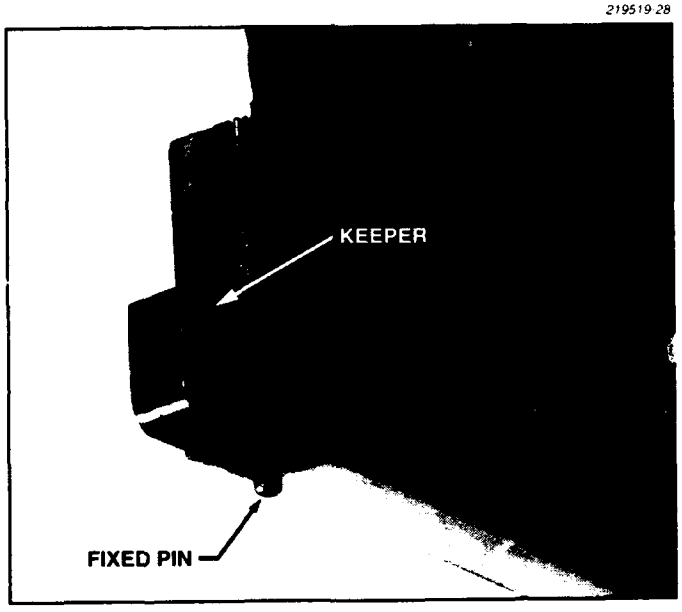

Figure 31. Reflector petal keeper, fixed pin.

This restraint system, cycled repeatedly for a number of months, began to show signs of failure. Some of the spring end-loops became deformed and separated from their pin grooves. This fatigue-related occurrence was corrected with redesigned pivot hardware and modified spring loops. The selected replacement pivot assemblies resemble two miniature flanged cylinders that are positioned base to base and joined in situ with the springs (equipped with double-looped ends) and petal, using a full-length, press-fit dowel (Figure 32).

With a suitable antenna rim restraint system in place, attention is now directed to the central clamping device. This assembly, mentioned earlier, consists of a threaded flanged tube (feed holder) and an oversized clamping nut. The original clamping nut had a keyed finger spring washer fitted to the underside, which was used as a preclamp petal retainer. A pair of tabs, bonded to the top surface, served as thumb pads. The threaded hub flange, which is the clamp base, contains a set of guide pins used to position the petal set.

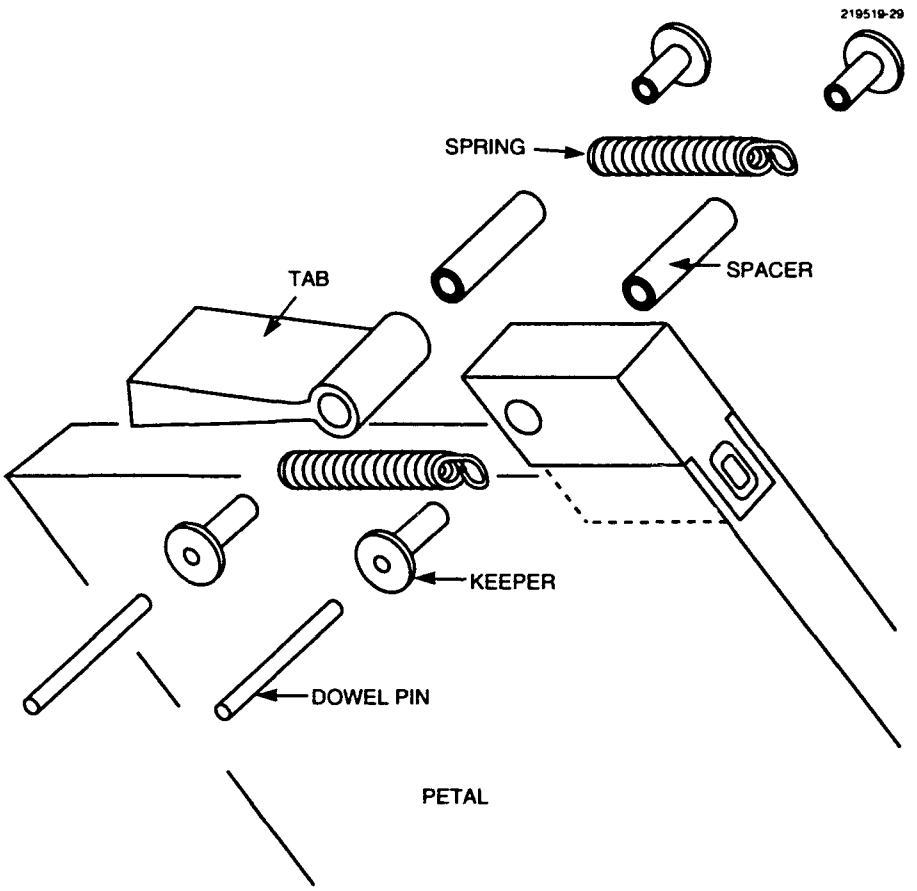

Figure 32. Exploded view of petal latch assembly.

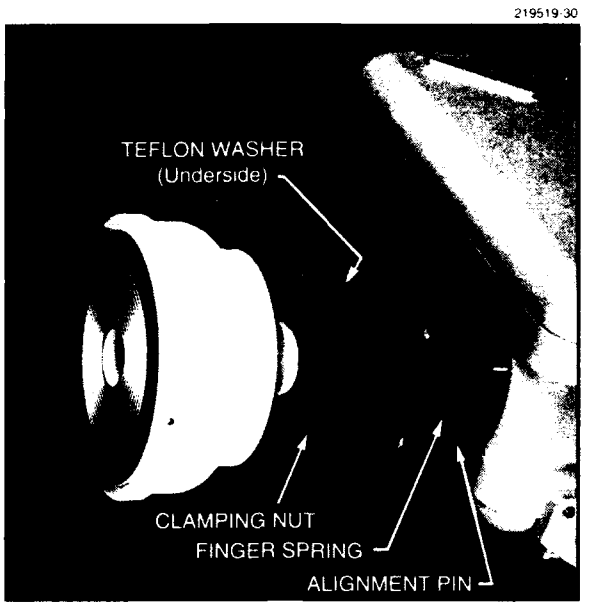

Figure 33. Reflector central clamp components.

The finger spring washer was redesigned due to its repeated binding at the key interface. Relocation of these spring pairs to newly created recesses in the hub flange eliminated any problems associated with the moveable spring assembly (Figure 33). The clamping nut could now be simplified, machined from a single blank, replacing the sharp-cornered, bonded tabs with formed ribs. A Teflon thrust washer was installed in the area once reserved for the spring washer.

The petal guide pins, referred to earlier, were enlarged to better withstand the anticipated petal insertion forces and provide a more robust positioning indicator. These pins (one per petal) engage the slot located on the underside of each petal tip. A fully inserted petal is seated against the hub cylinder and a pin is captured in its guide slot. When all six petals are positioned and the rim restraints and central clamp are actuated, the Advanced SCAMP antenna reflector (Figure 34) is established.

The ASCAMP feed external body design revolves around the compact port arrangement. This feature allows the use of a mounting scheme that resembles a threaded fastener and nut (Figure 35). A low assembly weight and ease of installation are added benefits of this system.

7.3 RADOME

Radome/subreflector assembly design involved several phases. Initially, a polyethylene radome was selected. The subreflector was attached using a radial pattern of screws (Figure 36). This assembly was then affixed to the feed at the threaded horn/radome interface. After a short period of use, the polyethylene was deemed too dimensionally unstable for its intended application.

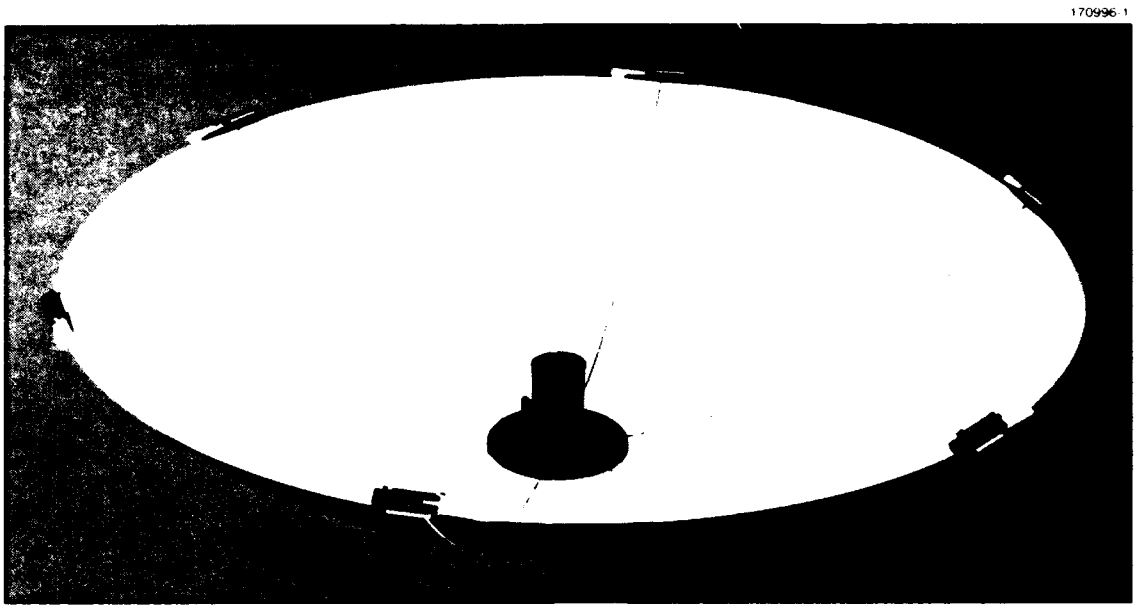

Figure 34. ASCAMP antenna reflector.

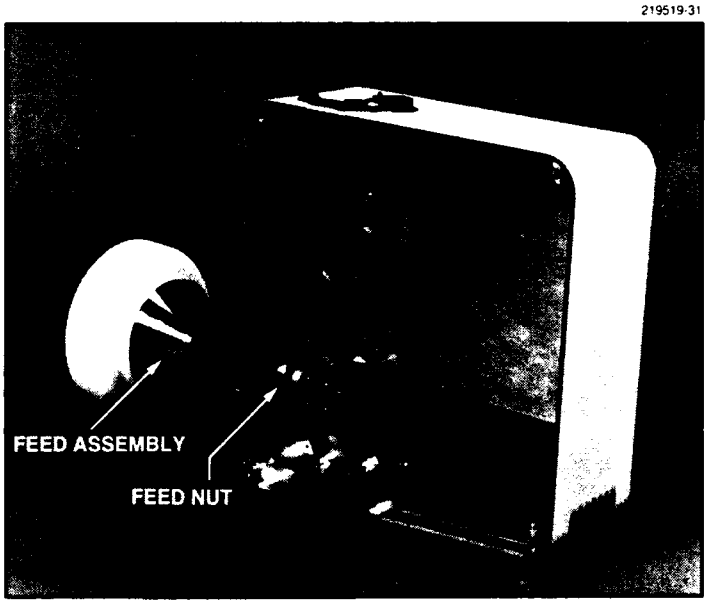

Figure 35. Feed assembly installation.

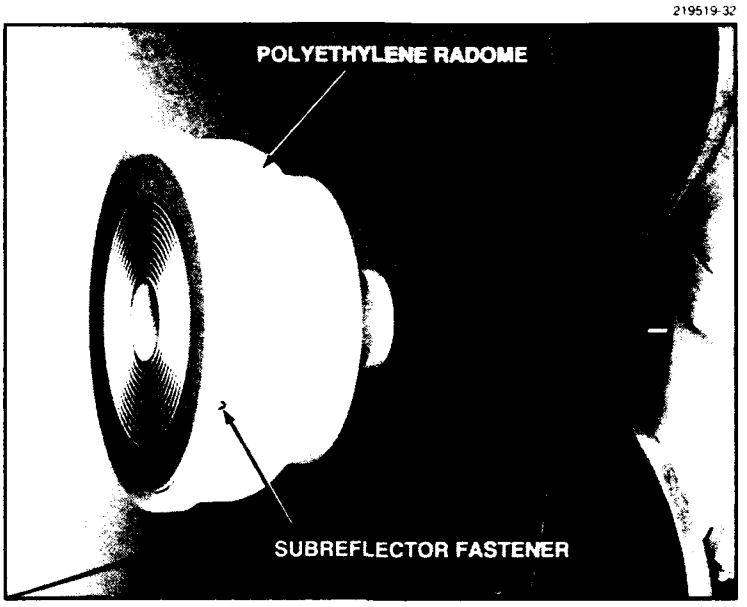

Figure 36. Radome/subreflector, mechanically attached.

Rexolite became the material of choice for the next radome design. The feed horn/radome threaded interface concept was retained with the addition of an environmental seal (O-ring). Changes did occur at the radome/subreflector junction. The method selected to unite the two items was a formed-in-place gasket bond. A pair of opposing shallow grooves were cut—one each in the subreflector and radome walls (Figure 37). Sealing compound was then introduced into the void created by the grooves.

Several Rexolite evaluation cylinders were assembled using different types of room temperature curing compounds. The test specimens were then placed in an environmental chamber for a two-week period and cycled twice daily from –30°C to 50°C. These temperature fluctuations would cause condensation on the internal surface if the seals are proved less than airtight. After passing the condensation test, the assemblies were immersed in water to further verify the integrity of the seals. The material possessing the most desirable performance characteristics proved to be a Hexcelite two-part urethane compound. This seal/bond configuration is the process used at the radome/subreflector interface (Figure 38).

After repeated terminal deployments, the threaded horn/radome interface seal was found to be unreliable. The remedy was to add a flange with mounting hole pattern to the feed horn rim. A matching pattern of threaded inserts was installed in the radome assembly base. This arrangement, when assembled with an O-ring seal, is the design employed currently (Figures 39 and 40).

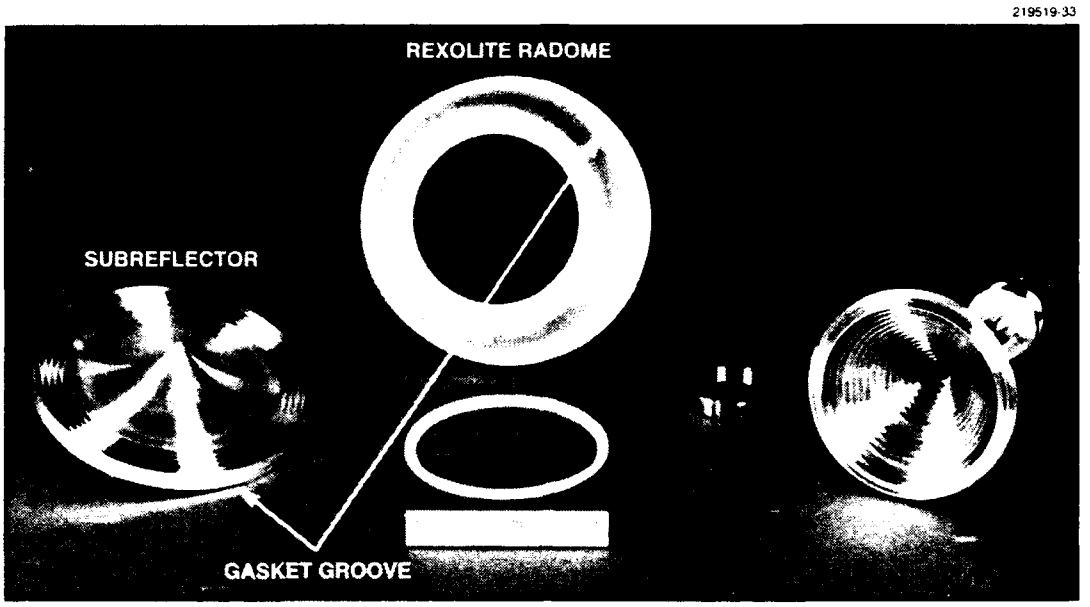

Figure 37. Radome/subreflector components.

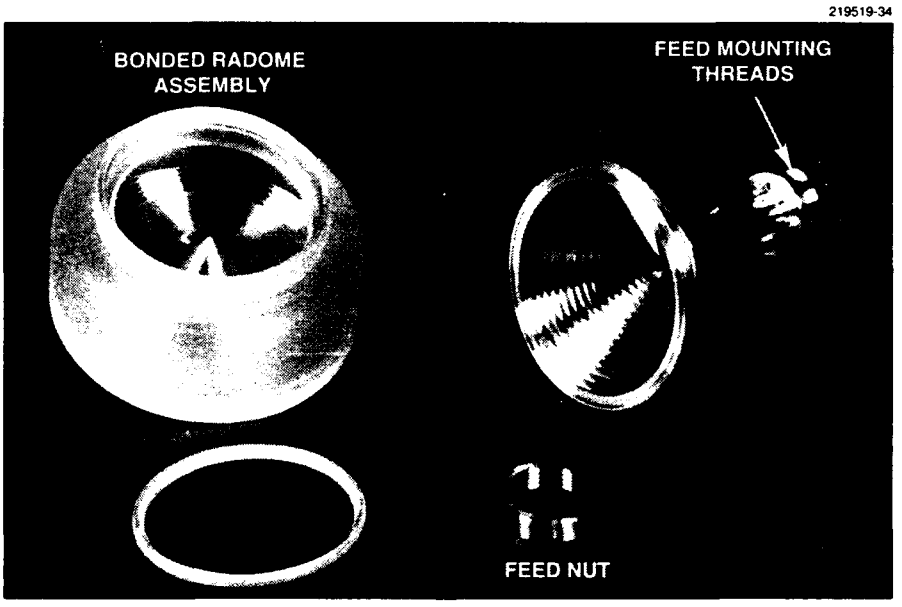

Figure 38. Radome/subreflector, bonded.

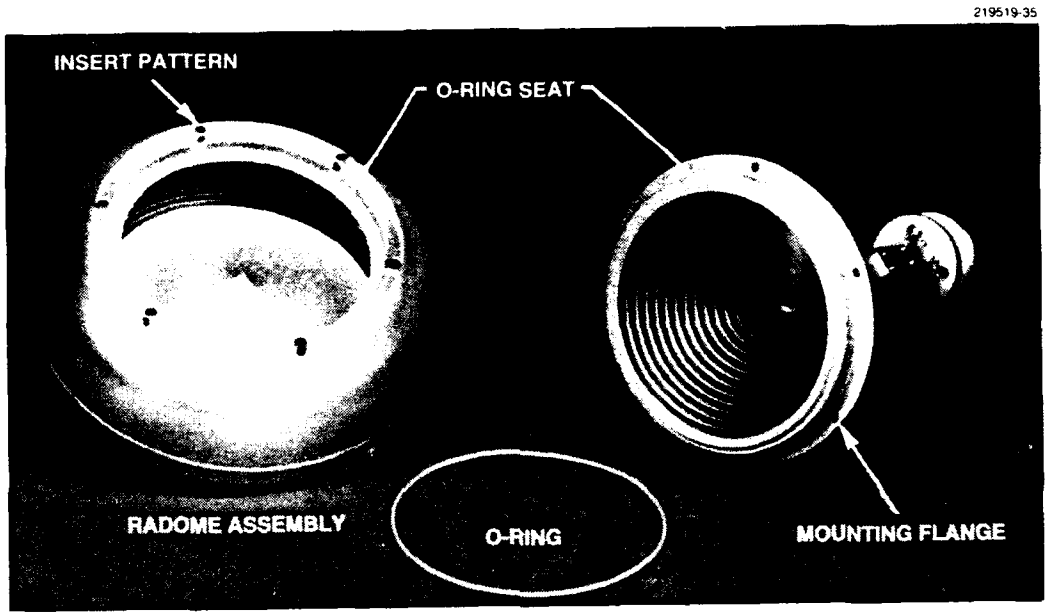

Figure 39. Feed/radome assembly, environmental interface.

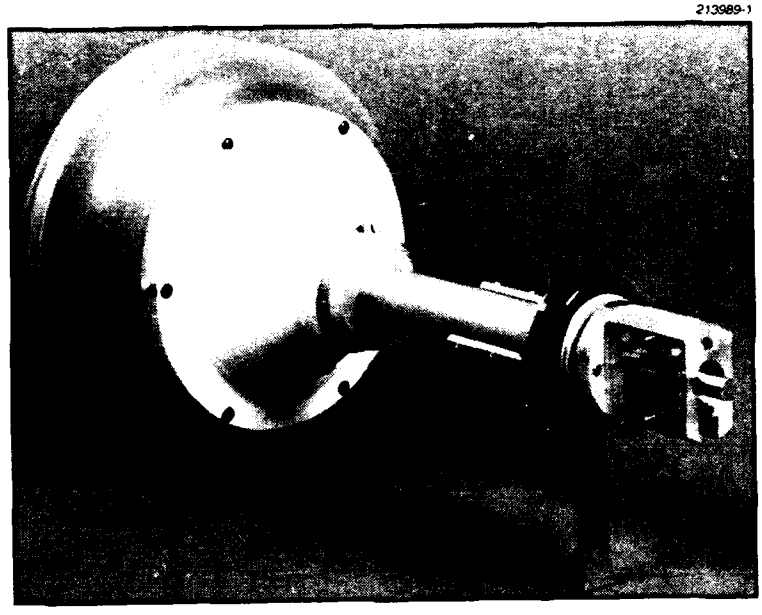

Figure 40. Dual-frequency feed assembly.

7.4 PAINT

The finishing phase of the feed assembly and antenna, as with the terminal structure, is an air-cured aliphatic polyurethane paint. Exposed metallic feed surfaces and the reflective antenna areas receive two and one coat(s), respectively. The selected paint is a two-part composition with tan pigmentation. A flatting agent is added to produce an abrasion resistant, lusterless coating, possessing a minimal visual signature.

8. CONCLUSIONS AND DISCUSSION

A compact, high performance, dual-band antenna system was developed for Advanced SCAMP, consisting of a compact feed with an elliptical subreflector, which produces a ring focus for a displaced axis parabolic reflector made up of six removable petals. This reflector represents a new approach to deployable antenna design. When fully tested and analyzed, it may be possible to modify the reflector shape and realize better overall antenna efficiency. Measurements of antenna gain deterioration as a function of petal surface and petal alignment irregularities are being made. Results will be reported separately.

The present satellite tracking method (which is relatively slow) used by ASCAMP is to mechanically step-point the whole antenna assembly. For applications that require higher tracking speed, the dual-band feed can be modified to provide an electronic lobing capability [11]. Four circumferentially located resonant cavities can be added at the coaxial waveguide opening of the dual-band feed. The coupling of these cavities to the K-band coaxial waveguide can then be controlled by a positive-intrinsic-negative semiconductor diode located at the open end of each of the four cavities.

REFERENCES

1. C.A. Lindberg, Private communication (meeting speech, 1984).

2. S. Klaus, "Hybrid design proves effective for flat millimeter-wave antennas," *Microwave System News & Communication Technology*, 123 (June 1985).

3. J.C. Lee, "A compact Q-/K-band dual frequency feed horn," *IEEE Trans. on Antennas Propag.*, 1108 (October 1984).

4. J.C. Lee, "Improvements in or relating to microwave aerials," U.K. Patent No. 973583 (1964).

5. Y.A. Yerukhimovich, "Analysis of two-mirror antennas of a general type," *Telecommunications and Radio Engineeering, Part 2*, 97 (1972).

6. Y.A. Yerukhimovich, "Development of double-reflector antennas with a displaced focal axis," *Telecommunications and Radio Engineering, Part 9*, 90 (1972).

7. G.Z. Aizenberg, V.G. Yampolsky, and O.N. Tereshin, "SHF antennas, Part II" (in Russian), Moscow: Svjaz Press (1977).

8. W.R. Rotman and J.C. Lee, "Compact dual-frequency reflector antennas for EHF mobile satellite communications terminals," *IEEE Int. Symp. Antennas Propag*, 771, Boston, Mass. (1984).

9. J.C. Lee, "Compact broadband rectangular-to-coaxial waveguide junction," U.S. Patent No. 4,558,290 (December 1985).

10. R.J. Figucia, "A timesaving acquisition procedure using sidelobe detection," *Milcom '91*, McLean, Va., 814 (November 1991).

11. J.C. Lee, "A dual-frequency feed with electronic tracking capability," Technical Report 779, Lexington, Mass.: MIT Lincoln Laboratory (May 1987), DTIC-AD-A182123.

REPORT DOCUMENTATION PAGE

Form Approved
OMB No. 0704-0188

1. AGENCY USE ONLY (*Leave blank*)	2. REPORT DATE	3. REPORT TYPE AND DATES COVERED
	22 September 1993	Technical Report

4. TITLE AND SUBTITLE

A Compact, Portable EHF/SHF Antenna for Advanced SCAMP

5. FUNDING NUMBERS

C — F19628-90-C-0002
PE — 33142A
PR — 584

6. AUTHOR(S)

Joseph C. Lee

7. PERFORMING ORGANIZATION NAME(S) AND ADDRESS(ES)

Lincoln Laboratory, MIT
P.O. Box 73
Lexington, MA 02173-9108

8. PERFORMING ORGANIZATION REPORT NUMBER

TR-981

9. SPONSORING/MONITORING AGENCY NAME(S) AND ADDRESS(ES)

PM Milstar (Army)
SFAE-CM-MSA
Building 909
Ft. Monmouth, NJ 07703-5508

10. SPONSORING/MONITORING AGENCY REPORT NUMBER

ESC-TR-93-211

11. SUPPLEMENTARY NOTES

None

12a. DISTRIBUTION/AVAILABILITY STATEMENT

Approved for public release; distribution is unlimited.

12b. DISTRIBUTION CODE

13. ABSTRACT (*Maximum 200 words*)

The small, single-channel, antijam, man-portable (SCAMP) terminal is used for extremely high frequency (EHF) satellite communication. Since its development in 1987, it has repeatedly demonstrated successful communication through the EHF packages on the FLTSAT-7 and -8 Navy communication satellites.

Advanced SCAMP is the second generation small terminal, highly elevated in performance and significantly reduced in weight. It is currently being developed at Lincoln Laboratory. Pertinent parameters are its 30-lb total weight, 75- to 2,400-bps data rate, and 24-in antenna aperture.

Starting with the basic dual-band feed developed for another application, a compact, high-performance, EHF, dual-band ring-focus feed with an elliptical subreflector was developed for a displaced axis parabolic reflector. This reflector is made up of six lightweight deployable petals for portability.

The feed weighs less than 1 lb, and the reflector weights 2.6 lb. The measured added loss due to imperfections of the petal reflector for the 44.5- and 20.7-GHz bands are 0.3 and 0.1 dB, respectively. An overall antenna efficiency of about 65% and 55% in the Q- and K-bands was achieved.

Antenna and feed design considerations, measured performance, and other possible applications for this antenna are discussed.

14. SUBJECT TERMS

dual-frequency band
deployable petal reflector
elliptical subreflector
advanced SCAMP
EHF/SHF
compact portable terminal
ADE
SCAMP
Q-band/K-band
displaced axis reflector
ring-focus feed
space communications
millimeter wave
antennas
corrugated horns

15. NUMBER OF PAGES
62

16. PRICE CODE

17. SECURITY CLASSIFICATION OF REPORT	18. SECURITY CLASSIFICATION OF THIS PAGE	19. SECURITY CLASSIFICATION OF ABSTRACT	20. LIMITATION OF ABSTRACT
Unclassified	Unclassified	Unclassified	Same As Report